Chapter 10

# Enhancement of Photoelectrocatalysis Efficiency by Using Nanostructured Electrodes

Guilherme Garcia Bessegato,
Thaís Tasso Guaraldo and
Maria Valnice Boldrin Zanoni

Additional information is available at the end of the chapter

http://dx.doi.org/10.5772/58333

## 1. Introduction

This chapter describes some fundamental features of photoelectrocatalytic processes, including the basic concepts of the technique, the phenomena at the electrode/electrolyte interface and the development of new materials employed in the last few years related to the specific applications. The nanostructured materials used in the photoelectrochemical field can be called photoanodes (n-type) when oxidation reactions take place at the interface, and photocathodes (p-type) when the reduction is the main process [1, 2]. This chapter focuses on photoanode materials and how their surface influences the applications of this technique.

Photoelectrocatalysis could be described as a multidisciplinary field, involving surface science, electrochemistry, solid-state physics and optics. The basic concept is that when a semiconductor surface is irradiated by light ($h\nu \geq E_g$) there is generation of electron/hole pairs ($e^-/h^+$) by the promotion of an electron from the valence band (lower energy level) to the conduction band (higher energy level). The electrons are forwarded to the counter electrode under positive bias potential (n-type) in order to minimize the recombination of these pairs due to the short life-time. When immersed in electrolyte the adsorbed water molecules and/or hydroxyl ions react with the holes on the valence band to generate hydroxyl radicals ($^{\bullet}OH$), which are a powerful oxidizing agent (+2.80 V) [3-5].

The first findings, from 1839, found that the photoelectrochemistry field was stimulated by the Becquerel effect [6]. They observed a photocurrent flow of electrons due to illumination of a material connected by two electrodes immersed in solution. In 1972, the work of Fujishima and Honda had a huge impact on this field. They studied the use of a $TiO_2$ semiconductor on the photoelectrolysis of water (water splitting) under anodic bias potential in a photoelectrochemical (PEC) cell [7, 8]. Nowadays, photoelectrocatalysis is an emerging field with many applications, such as organic compounds oxidation [9-11], inorganic ions reduction [12, 13], disinfection [14, 15] and production of electricity and hydrogen [16-18].

The development of this technique is intimately related to a better understanding of materials' surfaces and properties. Highly ordered nanomaterial arrays have promoted a revolution in applications of these materials as nanotubes, nanowires, nanofibres, nanorods, nanowalls, etc. [19]. The main applications of the technique include the degradation of unwanted environmental pollutants (organic and inorganic compounds) and converting sunlight directly into an energy carrier [4, 19, 20].

This work presents an overview of the fundamentals of photoelectrocatalysis and the huge contribution made by nanostructured architectures, as well as explaining the efficiency of the technique as a treatment method for organic and inorganic compounds and for water splitting.

## 2. Photoelectrocatalysis: Basic concepts

Advanced oxidation processes (AOPs) have been proposed as alternative methods for the degradation of recalcitrant organic compounds in water [21], air [22] and soil [23] in recent years [4]. AOPs are based on the generation of hydroxyl radicals ($^{\bullet}OH$) as highly oxidant species, which are responsible for the oxidation of the major pollutants [4, 21]. Among the AOPs, heterogeneous photocatalysis deserves particular attention [5]. The method is based on the use of a semiconductor (mostly $TiO_2$) irradiated with light energy equal to or greater than its band-gap energy. Since 1972 it has been known that is possible to promote photoelectrolysis of water (water splitting) under anodic bias potential [8]. Since then, photocatalysis has been explored to promote organics oxidation [9-11], inorganics reduction [12, 13], disinfection of water containing biological materials [14, 15] and production of electricity and hydrogen [16-18].

A semiconductor material is characterized by two energy bands separated by the band-gap energy, $E_g$. A semiconductor at absolute zero is insulating, because the valence band (lower energy level) is completely occupied and the conduction band (higher energy level) totally empty (Figure 1). To become conductive, charge carriers need to be created, usually by photoexcitation. The basic concept is that when a semiconductor surface is irradiated by light ($h\nu \geq E_g$) there is generation of an electron/hole pair ($e^-/h^+$) by promotion of an electron from the valence band (VB) to the conduction band (CB) (Equation 1) [5, 24].

The oxidizing nature of the holes ($h^+$) in the valence band means they generate $^{\bullet}OH$ radicals by the oxidation of $H_2O$ molecules or $OH^-$ ions adsorbed on the semiconductor surface, and are also able to oxidize organic molecules directly. The photoexcitation of $TiO_2$ and possible oxidation of an organic compound (RX) are represented in Equations 1–4 [21, 25].

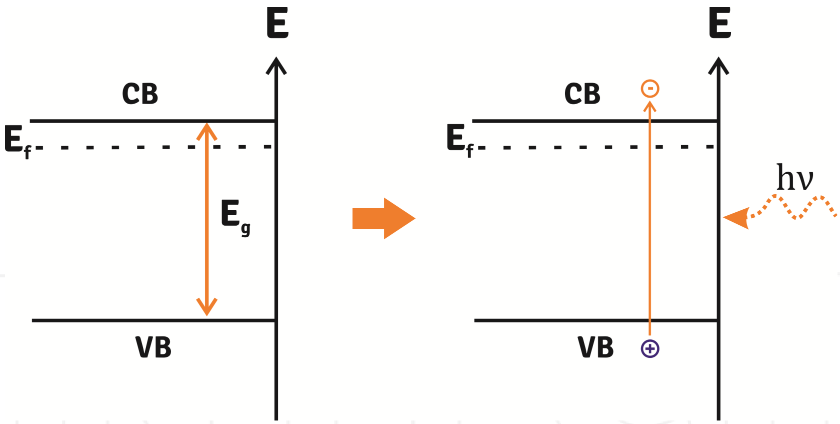

**Figure 1.** Schematic representation of the energy band diagram in a semiconductor and the mechanism of charge carrier generation by photoexcitation

$$TiO_2 \xrightarrow{hv} TiO_2 - e^-_{CB} + TiO_2 - h^+_{VB} \tag{1}$$

$$TiO_2 - h^+_{VB} + H_2O_{ads} \rightarrow TiO_2 - HO^\bullet_{ads} + H^+ \tag{2}$$

$$TiO_2 - h^+_{VB} + HO^-_{ads} \rightarrow TiO_2 - HO^\bullet_{ads} \tag{3}$$

$$TiO_2 - h^+_{VB} + RX_{ads} \rightarrow TiO_2 + RX^{\bullet +}_{ads} \tag{4}$$

Although heterogeneous photocatalysis is a well understood process, and despite its promising results in water decontamination, its practical exploitation has been restricted by its low photonic efficiency, which is mainly due to recombination of the $e^-/h^+$ pair, as shown in Equation 5 [25, 26].

$$TiO_2 - e^-_{CB} + TiO_2 - h^+_{VB} \rightarrow TiO_2 + heat \tag{5}$$

Therefore, there are considerable efforts being made to obtain new processes able to separate charge carriers and minimize their recombination rate [26, 27]. The combination of electrochemical and photocatalysis processes (photoelectrocatalysis) offers the opportunity to separate photo-generated $e^-/h^+$ pairs by gradient potential [28, 29]. Specifically, when the photocatalyst is attached to a conductive substrate (photoanode), there is the possibility to apply an anodic bias potential to the semiconductor and to modify the substrate/electrolyte interface. This alternative improves the efficiency of charge separation by driving the photogenerated electrons via the external circuit to the counter electrode [26, 28-30]. Figure 2 illustrates the mechanism of photoelectrocatalysis.

Furthermore, the great goal is to avoid the removal of photocatalyst suspensions. The immobilization of the photocatalyst particles on a solid substrate is usually applied on photoelectrocatalysis and therefore the process dispense next filtration step [28, 29].

It is interesting to understand why photoelectrocatalysis is efficient in charge separation. When a semiconductor is in contact with an electrolyte there is formation of a junction semiconductor/electrolyte interface, which determines the electron hole separation kinetics. The junction in a redox electrolyte causes a change in the electrochemical potential (Fermi level) due to discrepant potentials at the interface [19]. Thus, the equilibration of this interface needs the flow of charge from one phase to another, and a band-bending is created within the semiconductor phase. The amount of band-bending in this Schottky junction will depend on the difference of the Fermi levels of semiconductor and electrolyte. The region where there is bending is called the space charge layer (SCL), which is characterized by the accumulation of electrons or holes at the surface [5, 19, 24, 31]. Figure 3 shows the behaviour of these charges in the semiconductor before and after this equilibration when it is in contact with an electrolyte.

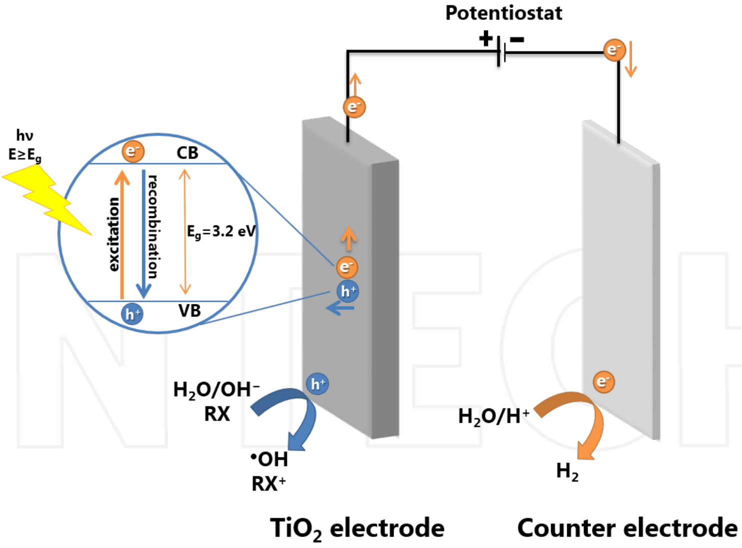

**Figure 2.** Schematic representation of the mechanism of separation and recombination of charges in the photocatalysis or photoelectrocatalysis and mechanism of charge separation in a photoelectrochemical system, where a gradient of potential is created

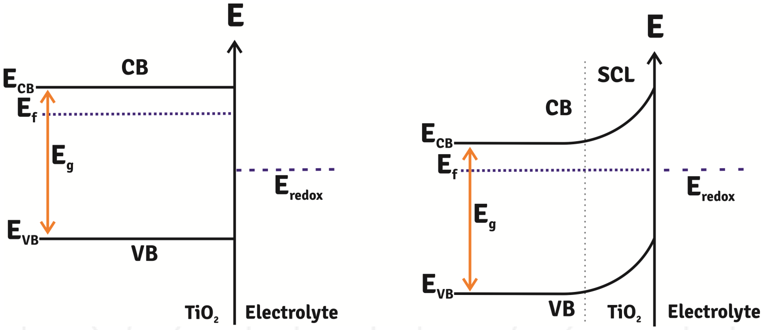

**Figure 3.** Energy band diagram for an n-type semiconductor before and after the equilibration of Fermi levels at the interface semiconductor/electrolyte, and the appearance of band-bending and the space charge layer (SCL)

Another method to control the Fermi level (and therefore the band-bending) is by applying a bias potential [19]. For any given semiconductor and electrolyte, there is an exact potential for which the potential drops between the surface and the bulk of the electrode is zero; in other words, there is no space charge layer [31]. Because the band edges are flat, this potential is called flat-band potential, $V_{fb}$ (Figure 4). The application of any potential greater than the flat-band potential will increase the band-bending at the n-type semiconductor electrode, such as $TiO_2$. In this case electrons are depleted and holes enriched at the surface, as we can see in Figure 4. When $TiO_2$ is irradiated, it is observed that the photogenerated holes have an oxidizing power equivalent to the potential of the valence band edge, and are able to oxidize an RED molecule, whose formal potential is more negative than the valence band. In the case of $TiO_2$, the $H_2O$ can be oxidized producing $^{\bullet}OH$ radicals. The electron in the conduction band flows via an external circuit to the counter electrode, where reduction reactions may occur, such as the reduction of $H^+$ ions to $H_2$ (Figure 2). It is important to note that in photo(electro)catalysis, the greater the band-bending (and therefore the SCL) the faster the electron/hole separation occurs, and then the recombination of charges is minimized [5, 19, 24, 31].

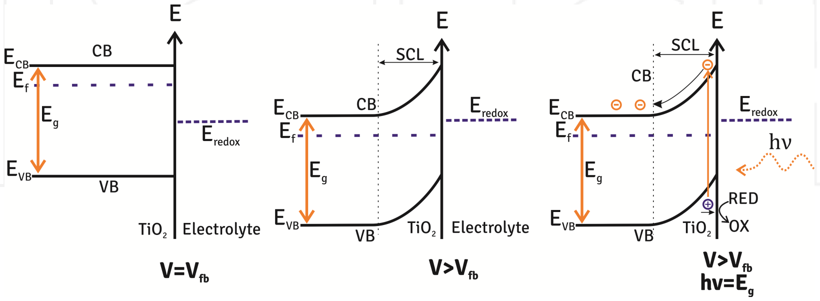

**Figure 4.** Energy band diagram for a n-type semiconductor when the applied potential (V) is equal to flat-band potential ($V_{fb}$) and when the applied potential (V) is greater than $V_{fb}$. The last schematic shows the mechanism of charge separation when the electrode is submitted for a potential higher than the $V_{fb}$ and irradiated with $\lambda \geq E_g$.

Thus, considering the high oxidative power of $^{\bullet}OH$ that is easily generated by irradiation of the $TiO_2$ surface, an increased number of applications of photoelectrocatalysis has developed with the aim of promoting the degradation of organic pollutants to $CO_2$ and minerals.

## 3. The degradation of organic compounds on thin films

The presence of recalcitrant organic pollutants such as pesticides, hormones, pharmaceuticals, phenols, surfactants and dyes in water and wastewater has been described in the literature as one of the most serious problems for human beings and the environment [32, 33]. The great concern is mainly that the genotoxic and mutagenic properties of these pollutants can cause bioaccumulation problems and transportation that is magnified in the food chain [34]. They have therefore received great attention since they are released into the environment through a variety of human and industrial activities. Conventional techniques such as adsorption, precipitation, flocculation and reverse osmosis simply transfer organic pollutants from different phases or concentrate them in one phase, without actually removing them [33].

Different methodologies have been proposed to promote the complete degradation of organic matter. Among them, the use of advanced oxidative processes (AOPs) has been seen as an efficient alternative for pollutant degradation and has received a great deal of attention from several researchers. The *in situ* generation of hydroxyl radicals ($HO^{\bullet}$) has proved effective in the oxidation of most organic substances because it is both a non-selective reagent and a highly oxidizing agent [21]. However, the complete mineralization which is the conversion of organic molecules into $CO_2$, $H_2O$ and other small molecules, the reaction mechanisms and the characterization of secondary products and intermediates have not been frequently investigated [35].

Over the past decades, electrochemical methods such as electrocoagulation, electrocatalysis oxidation and reduction, electro-Fenton, photoelectro-Fenton, photocatalysis and photoelectrocatalysis (Figure 5) have been pointed out as good alternatives to promote the degradation and mineralization of organic pollutants, since they combine the advantages of hydroxyl radicals formation and the efficiency of electrochemistry [21, 36].

In Electrochemically Mediated Oxidative Advanced Processes (EOAPs), hydroxyl radicals can be generated by direct electrochemistry (anodic oxidation) or indirectly through electrochemical generation of Fenton's reagent. In photoelectrocatalytic oxidation the $^{\bullet}OH$ is generated heterogeneously by direct water discharge on specific anodes such as DSA and BDD electrodes [36]. During the electro-Fenton reaction the hydroxyl radicals are generated homogenously via Fenton's reaction [37].

Photoelectrochemical methods have been intensively investigated as promising alternative methods not only to remove organic pollutants but also to decrease toxicity, since they degrade substances in a short period of time. The degradation mechanism of photocatalysis can be classified into five steps: (1) transfer of reactants in the fluid phase to the surface; (2) adsorption of the reactants; (3) reaction in the adsorbed phase; (4) desorption of the products; and (5) removal of products from the interface region [38].

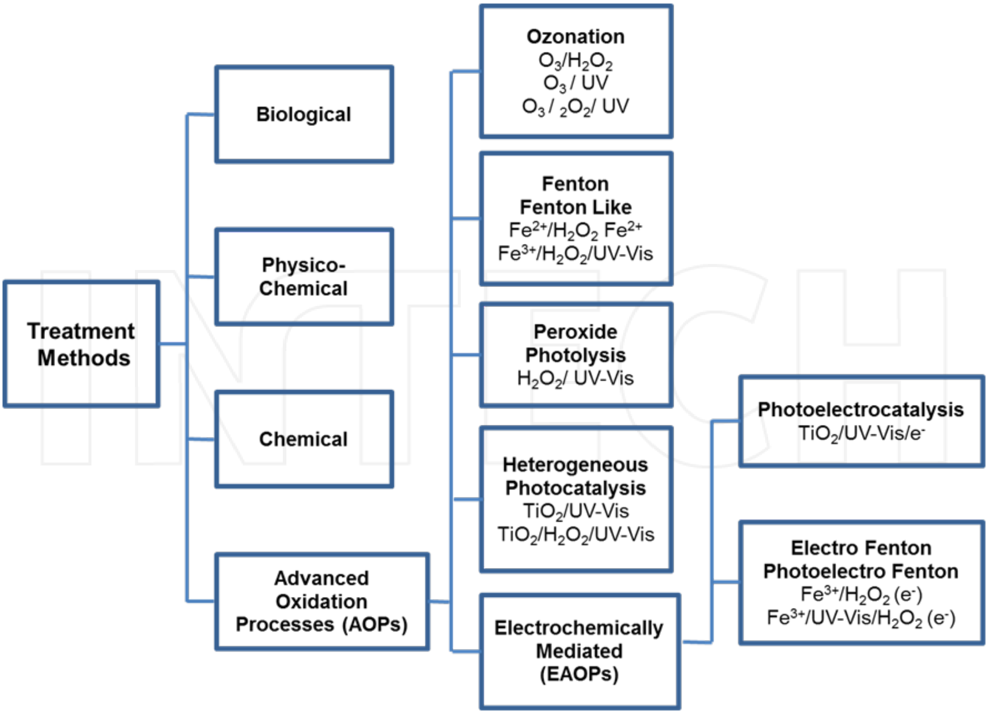

**Figure 5.** Treatment methods described for the degradation of organic pollutants, including conventional techniques and advanced oxidation processes

The key to obtaining success with photocatalytic and photoelectrocatalytic methods is the development of novel efficient materials as working electrodes, which present good optical, mechanical, electronic, electrochemical and catalytical properties [39]. The choice of the synthesis method to produce the semiconductor material is of fundamental relevance, as it will determine the efficacy of the PEC treatment. All factors related to the surface material will influence the success of photoelectrochemical processes as morphological and structural features (particle size, surface area), good charge separation ($e^-/h^+$), suitable photonic efficiency and band-gap energy level [40].

### 3.1. Synthesis of thin film semiconductor materials

Emerging technologies providing feasible alternatives for the development of new materials have been the subject of several studies. Titanium dioxide is the most used material and can be prepared in the form of powder, crystals or thin films. To obtain good-quality materials there are many methods described in the literature, based on precipitation and co-precipitation [41, 42], solvothermal [5], sol-gel [43], microemulsion [44], electrochemical [40] and gas-phase methods [40].

Heterogeneous photocatalysis started with the use of $TiO_2$ semiconductors in a slurry system (suspension of fine powder). The most efficient powder reported in the literature is the Degussa P25, which is a combination of rutile and anatase allotropic phases in the ratio 3:1. There are many advantages of using this powder: it provides high surface area showing excellent photocatalytic activity because of the adsorptive affinity of organic compounds on the surface of anatase [45]. However, a post-treatment filtration step is required to separate it from the solution, which limits practical application as this is a time-consuming and costly process. Moreover, the suspended particles tend to aggregate, especially at high concentrations, which makes the separation more complicated and limits application in continuous flow systems [46].

Since 1993, the immobilization of $TiO_2$ on a substrate has offered an alternative way of using powder and started a search for thin films [28, 47]. Several researchers have anchored photocatalysts onto a variety of surfaces, such as glass (ITO and FTO), silica gel, metal, ceramics, polymer, thin films, fibres, zeolite, alumina clays, activated carbon, cellulose, reactor walls and others [33]. To support $TiO_2$ there must be four main criteria: strong adherence, stability of the catalyst, high specific surface area to promote strong adsorption of the pollutant on the electrode surface [38]. The substrate material has a great influence on the electron transfer along the film. It is reported that conducting glasses have a relatively poor connection within the film; on the other hand, metal substrates present a lower impedance because there is a reduction of charge transfer resistance leading to better PEC activity [33].

The photocatalytic activity of a $TiO_2$ system mainly depends on its intrinsic properties, such as particle size, surface area, film thickness, crystallinity and crystal phase [33, 48]. For this purpose, many different techniques emerge from the need for immobilization, since the photocatalytic activity of the film is highly dependent on the preparation method [46]. For instance, the most reported preparation routes are sol-gel [43], chemical vapour deposition [49], electrodeposition [50], sol-spray [51], and hydrothermal [38]. Besides the preparation routes, the coating techniques also influence the resulting material properties. Deposition methods such as dip-coating [52], spin coating [53] and even the development of new coating methods based on conventional dip and spin coating [54] have been shown to be simple and able to produce stable materials.

When compared to other methods, the advantages of the sol-gel technique are easy control of deposits, reliability and reproducibility, resulting in good-quality nanostructured thin films [55]. In fact, successful formation of the desired crystal phase is directly related to the starting material, composition, and deposition, as well as the annealing temperature. The crystal morphology has a direct relation to the light absorption as incident light affects photoelectrocatalytic efficiency. Film thickness can affect the efficiency of both light energy conversion and electron transfer; thick films may lower efficiency as these processes have a higher resistance [33]. It has been also shown that the pH of the original solution can influence particle size [56]. It is known [56] that acidic conditions favour the formation of smaller particles, while at higher pH values larger particle size is observed. The use of sol-gel methods has inspired a great number of studies on the development of new semiconductors for the suppression of electron/hole recombination and enhancement of the photosensitivity of titania for successful application [57]. Therefore, the use of nanoporous thin films for photoelectrochemical purposes has been widely described in studies on the removal of organic matter such as dyes [58], phenol [59], tetracycline [60], toxic metals [61] and microorganisms [62]. Annealing temperature has been intimately related to the crystal structure formation because phase transfer is temperature dependent. For many uses, including photoelectrocatalysis and solar cells, the most desired crystal structure is anatase, because this structure shows a higher charge carrier mobility than rutile [19, 63]. However, in many cases of photocatalysis, combinations of anatase and rutile have been used due to the higher photocatalytic activity that these display compared to pure anatase (probably due to the smaller band-gap energy of rutile ($E_g$=3.0 eV vs. anatase $E_g$=3.2 eV) absorbing more visible light radiation).

The use of mesoporous $TiO_2$ thin films has also been studied. According to the definition of IUPAC, porous solids can be classified into three groups based on their pore diameter, namely microporous (5–20 Å), mesoporous (20–500 Å), and macroporous (>500 Å) materials [64]. The success of mesoporous materials depends on the availability of precursor materials and the precision of control over the hydrolysis reaction, as well as the choice of an appropriate surfactant. All these parameters interfere with the obtaining of highly organized materials. In order to obtain mesoporous materials with good photocatalytic features it is necessary to use an appropriate method to produce films with a large surface area, pore-wall structure and crystallinity [65].

Other thin-film semiconductors have been used in the degradation of such organic compounds as $WO_3$ [66], ZnO [67] and $Fe_2O_3$ [68, 69]. The anodic growing of tungsten trioxide thin film has been described as a good alternative to $TiO_2$, mainly because of its intrinsic characteristics like lower band-gap energy of $E_g$=2.8−3.0 eV and higher photoactivity [70]. Iron oxide ($\alpha$-$Fe_2O_3$) has the desirable property of narrowing the band gap ($E_g$=2.2 eV), as well as low cost, electrochemical stability and low toxicity [68]. ZnO ($E_g$=3.2 eV) has good properties for use as a photocatalyst, such as high photocatalytic efficiency, low cost and environmental friendliness [71]. It can also be used for degradation and disinfection purposes, as it can degrade dirt and inhibit the growth of microorganisms [67].

### 3.2. Operational characteristics on the PEC systems

The basic photoelectrochemical reactor setup consists of three conventional electrodes (working, reference and counter electrode) immersed in an aqueous electrolyte contained within a vessel for the potentiostatic mode. A two-electrode system (working and counter) can also be used when current density is used to supply the system. The vessel containing the aqueous electrolyte is transparent to light or fitted with an optical window, usually quartz, that allows light to reach the photoactive electrode [72].

Besides material properties, some operational parameters such as pH, biased potential, initial concentration of analyte and electrolyte composition have a direct influence on the degradation of organic pollutants. The point of zero surface charge (pzc) of the $TiO_2$ at the electrode/electrolyte interface will determine the adsorption of the pollutant in relation to the pH and pKa of the pollutant. In acidic conditions $TiO_2$ is positively charged, while in basic conditions it is negatively charged, according to the equations below [25, 33, 73]:

$$TiO_2 + H^+ \rightarrow TiOH_2^+ \tag{6}$$

$$TiO_2 + OH^- \rightarrow TiO^- + H_2O \tag{7}$$

The influence of biased potential on the degradation rate must be optimized as a function of the flat band potential. Generally, when the potential is increased, the degradation rate increases as well until no more gain is observed because electrons and holes have a good separation and recombination rate is minimized [33, 74]. Current density can be applied instead of potential, as it requires a much simpler arrangement of two electrodes, lowering costs and favouring the photoelectrocatalytic application on large-scale reactors [4, 43].

The initial pollutant concentration, especially for wastewaters and coloured solution, will limit the photoanode activation by light [61]. Moreover, at high concentration the photoelectrochemical efficiency is decreased and longer treatment periods will be required to achieve complete pollutant removal. Depending on the pollutant, it is possible to promote the degradation at high concentrations [4, 25].

Recent investigations prove that light intensity and lamp irradiance are critical factors in photoelectrochemical systems. It has been reported in the literature that the higher light intensity achieved, the faster the degradation rate will be [33]. Zainal and colleagues [75] demonstrated that a 100 W UV lamp was almost equivalent to a 300 W halogen lamp, probably due to the higher intensity of the halogen lamp.

When the degradation is conducted in the presence of different electrolytes, there will be significant change in the degradation rate. In the presence of chloride, the degradation is improved because there will be generation of chlorine radicals, with a high oxidizing power which is not observed in sulphate and nitrate mediums [58].

The PEC reactor also plays an important role in the efficiency of photoelectrochemical methods. Different materials (glass, quartz and Teflon) and shapes are employed on these systems. The photoanode irradiation can be used either externally or internally [4]. The reactor could be rectangular or cylindrical, although the latter makes greater use of light and hence better performance. There are single chamber reactors and double-vessel reactors, also known as H-type [72].

## 4. Strategies to enhance the PEC efficiency

Several photocatalysts have been applied in photoelectrocatalysis, among them $TiO_2$, $WO_3$ [66], ZnO [67], CdS, $Fe_2O_3$ [68, 69] and $SnO_2$. Over the years considerable effort has been devoted to the improvement of the materials used in photocatalysis. $TiO_2$ has become one of the most common materials used in materials science [20] as it is environmentally friendly, low cost, has a long lifetime of electron/hole pairs, presents a compatible energy position of BV and BC, and has good chemical and thermal stability and superior catalytic stability [20, 76]. Among these features, the band edge positions relative to $H_2O$ oxidation represent a very important characteristic that improves the applicability of $TiO_2$ in photo(electro)catalysis to decompose $H_2O$ to $H_2$ and $O_2$ and also to create $^{\bullet}OH$ radicals [19]. There are many transition metal oxides with semiconductor properties, but many of them do not have suitable electronic properties (energy position of bands edges) for useful electron transfer reactions.

Some of the main applications of $TiO_2$ photoelectrocatalysis have involved water-splitting [16, 77, 78] inactivation of microorganisms [14, 79] and degradation of contaminants in water [10, 33, 39, 78, 80]. Although it is the most suitable material for such applications, titanium dioxide has some limitations that hinder its use in technological applications. For example, it is activated only under ultraviolet irradiation ($\lambda \leq 387$ nm), and thus the use of sunlight is limited because it provides up to 5% of UV light; it also presents recombination of electron/hole pairs. In order to obtain a better utilization of the photocatalytic properties of $TiO_2$ and to achieve more responsiveness to the visible wavelengths, the preparation of nanostructured materials and their surface modification or doping (band-gap engineering) has emerged as a potential method.

Thus, in order to increase the efficiency of photoelectrocatalysis, organized nanostructured materials, especially those involving electrochemical methods of preparation, have attracted attention. The main advantages are discussed below.

### 4.1. Nanostructured morphologies

Nanostructured materials represent an important challenge of current science, and the new materials have presented special physical and chemical properties. Recently, one-dimensional (1D) nanostructures such as rods, belts, wires and tubes have become a focus of intensive research, mainly due to their high surface area (ideal for catalysis as it facilitates reaction/ interaction between the devices and the interacting media) and other exceptional properties such as electrical properties: charge carrier transfer is mainly governed by the quantum confinement phenomenon [81].

The discovery of carbon nanotubes by Iijima in 1991 [82], with their variety of interesting properties, boosted research focused on the synthesis of tubular nanostructures of other materials. Among the various nanotube materials, titanium dioxide nanotube arrays are of particular interest because of their many applications, for example in photo(electro)catalysis [10, 78, 83-87], sensors [88, 89], biosensors [90], dye-sensitized solar cells [91, 92], hydrogen generation by water photoelectrolysis [77, 78, 93], photocatalytic reduction of $CO_2$ [94, 95] and biomedical-related applications [96, 97].

In recent years, a great number of investigations have focused on the photocatalytic activity of $TiO_2$ nanomaterials and effective ways to improve their photocatalytic efficiency. Various nanostructures have been reported, such as nanowires [98], nanofibres [99], nanorods [100, 101], and nanowalls [101], but $TiO_2$ nanotubes are certainly the most promising and explored architecture.

### 4.1.1. $TiO_2$ nanotube arrays

As previously mentioned, $TiO_2$ is a widely studied materialdue to its versatility, and in photoelectrocatalysis it is undoubtedly the most explored semiconductor. The use of the $TiO_2$ nanotubes morphology has allowed advances in photo(electro)catalysis due to specific improvement of properties and will be further discussed.

For photoelectrocatalytic applications $TiO_2$ nanotubes ($TiO_2$ NTs) present interesting properties, such as large internal surface area, which can be easily filled with liquid enabling intimate contact with electrolytes and excellent charge transport [39, 94]. Due to its high structural organization, the nanotubes architecture exhibits excellent electron percolation pathways for vectorial charge transfer between interfaces, thereby minimizing the recombination of charges. Figure 6 illustrates an image of scanning electron microscopy (SEM) of $TiO_2$ NTs prepared under electrochemical anodization. As the $TiO_2$ film grows on the metal surface (is not deposited) there is a good electrical connection between the oxide and the metal. Zhu and colleagues [102] found charge carrier recombination much slower in the $TiO_2$ NTs films than in the nanoparticulate $TiO_2$ films in dye-sensitized solar cells.

Additionally, the morphological parameters of the architecture can be precisely controlled when the material is prepared by electrochemical anodization. The control of the nanotube dimensions is important because each application may require morphological surfaces with particular characteristics. For example, Liu et al. [103] found that the photoelectrocatalytic activity shows a dependence on the length of the nanotube arrays. They studied the degradation of phenol at $TiO_2$ NTs electrodes with different tube lengths under UV irradiation and applied potential. It was verified that a short nanotube array shows better photoelectrocatalytic activity than a long nanotube array, which can be explained by the reduced recombination effects. However, the photocatalytic degradation (no applying potential) showed that longer nanotubes were more efficient because they favour light trapping.

More information can be obtained in some excellent reviews found in the literature, dealing with preparation, properties, strategies to increase the photoactivity and applications of $TiO_2$ NTs [19, 20, 39, 81, 94, 104-107]. Titania nanotubes can be synthesized in two forms: powder form and self-organized nanotube arrays grown on a substrate of metallic titanium. Several techniques for the preparation of $TiO_2$ NTs have been reported, such as hydro/solvothermal methods [108], sol-gel [109], template-assisted methods [110] and electrochemical anodization [39, 105, 106]. The growth of $TiO_2$ NTs by electrochemical anodization in a fluorinated-based electrolyte is less expensive and simpler that most of these methods and allows precise control of dimensions, presenting a more orderly arrangement of nanotubes [105].

The first self-organized oxide obtained by anodization in electrolytes containing hydrofluoric acid was reported by Zwilling and colleagues in 1999, where a nanoporous structure was achieved [111]. In 2001, Gong and colleagues [112] developed the first generation of highly ordered and vertically oriented nanotube arrays of 500 nm length. The structure was obtained by electrochemical oxidation of titanium in a HF aqueous electrolyte. The fabrication of $TiO_2$ NTs films was performed in a two-electrode electrochemical cell using aqueous electrolytes

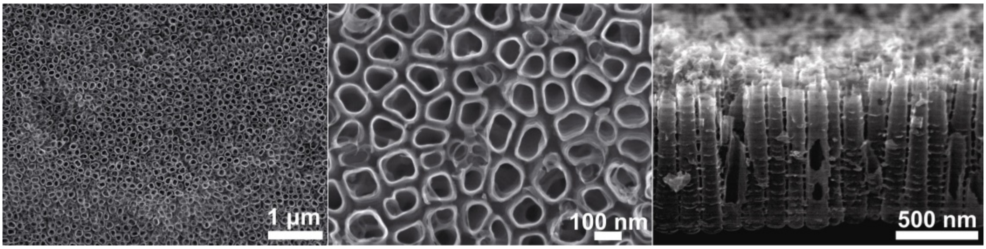

**Figure 6.** $TiO_2$ nanotubes scanning electronic microscopy (SEM) images, top view (in different magnifications) and cross section. The $TiO_2$ NTs were grown by electrochemical anodization of Ti foil in 1 M $NaH_2PO_3$+0.3 wt.% HF. The $TiO_2$ NTs presented a diameter of 110 nm, wall thickness of 13 nm and length of 900 nm on average

containing 0.5-3.5 wt. % HF and voltages varying from 3 to 23 V. They found that at low voltage (3 V), porous films are obtained and at higher voltage (23 V) the nanotube structure was destroyed. The ideal conditions were 0.5 wt. % HF electrolyte applying 20 V for 20 min.

In 2005, Cai and colleagues [113] developed the second synthesis generation of titania nanotubes. They found that adequate control of the electrolyte pH can decrease the oxide chemical dissolution rate; thus, the tube length is enhanced using aqueous buffer electrolyte. The pH of a KF-containing electrolyte is adjusted to 4.5 using additives such as sulphuric acid, sodium hydroxide, sodium hydrogen sulphate, and/or citric acid. This usually obtains $TiO_2$ NTs of 4.4 μm in length.

The third synthesis generation of titania nanotube arrays, initially reported by Ruan and colleagues [114] in 2005, involves improvements in nanotube-array length using non-aqueous electrolytes or polar organic solvents such as formamide, N-methylformamide, dimethyl sulphoxide, and ethylene glycol mixed with HF, $NH_4F$ or KF to provide fluoride ions [112, 115-117]. Ruan and colleagues [114] also studied the anodization of titanium in polar organic solvent using mixtures of dimethyl sulphoxide (DMSO) and hydrofluoric acid. $TiO_2$ nanotube arrays of 2.3 μm length were obtained in DMSO+4.0% HF electrolyte applying 20 V for 70 h.

The fourth synthesis generation of $TiO_2$ NTs was developed by Richter and colleagues [118] and Allam et al. [119], and is characterized by the fabrication of nanotube arrays by Ti anodization using fluoride-free HCl aqueous electrolytes. The mechanism of $TiO_2$ NTs formation on Ti substrate is well studied in the literature [94, 105, 106].

#### *4.1.1.1. Mechanism of formation of nanotubes by electrochemical anodization*

The production of oxide films on metal surfaces by oxidation in an electrolytic process can be called electrochemical anodization. In practice, a metallic electrode compatible with oxide growth is connected to the positive pole (anode) of a dc power supply and the cathode, usually a platinum piece (or another material, such as carbon for example) is connected to the negative pole (Figure 7). The electrodes are placed in an electrolytic solution and when a potential is applied in the system the metal reacts with oxygen ions from the electrolyte, growing an oxide film on the surface. The electrons resulting from the oxidation travel through the external circuit to reach the cathode, where they can react with $H^+$ ions and generate bubbles of $H_2$ [94]. The key point that determines the form of the oxide is the composition of the electrolyte. The $TiO_2$ NTs, in this case, can be achieved in electrolytes containing fluoride ions, with adjustments of applied potential and anodization time.

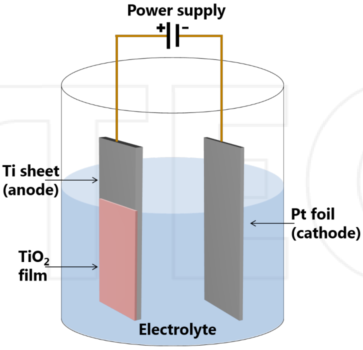

**Figure 7.** Scheme representing an electrochemical cell used to produce $TiO_2$ films by anodization of Ti

The growth of self-organized $TiO_2$ NTs (as well as porous structures of other metals such as Zr, Nb, W, Ta, and Hf) by electrochemical anodization in fluoride-containing electrolyte is governed by competition between steps that occur simultaneously.

First, there is the formation of oxide on the metal surface. In this step, there is a field-assisted oxidation of Ti metal to form $Ti^{4+}$ species which will react with $O_2^-$ (from $H_2O$). After the formation of an initial oxide layer, further oxide growth is controlled by field-assisted ion transport, where $O_2^-$ anions migrate through the oxide layer until they reach the metal/oxide interface, where they react with the metal [94, 106, 120].

$$Ti + 2H_2O \rightarrow \mathrm{TiO_2} + 4H^+ + 4e^- \tag{8}$$

In another step, $Ti^{4+}$ ions migrate from the metal through the oxide by field-assisted transport until they reach the oxide/electrolyte interface. Then, small pits are formed due to the localized dissolution of the oxide by the high electrical field, which act as pore-forming centres.

The key step is the chemical dissolution of oxide by fluoride ions at the as-formed pits, forming soluble fluoride complexes. The $Ti^{4+}$ ions field transported at the oxide/electrolyte interface are also complexed [94, 106, 120].

$$\mathrm{TiO_2} + 6F^- \xrightarrow{\mathrm{H^+}} \left[TiF_6\right]^{2-} + H_2O \tag{9}$$

$$Ti^{4+} + 6F^- \rightarrow \left[TiF_6\right]^{2-} \tag{10}$$

If the chemical dissolution is too high or too low, there is no formation of nanotubes. The dissolution rate can be adjusted by varying the concentration of $F^-$ and pH (more acidic pH and higher concentrations of $F^-$ increases the chemical dissolution) [94]. This was the principle used to obtain longer and smoother nanotubes, leading to the second and third generations of $TiO_2$ NTs.

When the rate of pore growth at the metal–oxide interface becomes identical to the rate of oxide dissolution at the pore–bottom–electrolyte interface, the thickness of the barrier layer remains unchanged, although it moves further into the metal, making the pore deeper [94, 106, 120]. Commonly, the wall thickness of $TiO_2$ NTs varies from 5 to 30 nm and the pore size from 20 to 350 nm (tube diameter is reported to be linearly dependent on the applied anodic potential during growth [106, 121]). The length often varies from 0.2 to 1000 μm; the aspect ratio, defined as the ratio between length and diameter of the tube, can be controlled from about 10 to approximately 20,000 by selection of appropriate anodization variables [94].

### *4.1.2. Nanostructured arrays of other semiconductors*

Nanostructured architectures are also fabricated by electrochemical anodization for other semiconductors of interest in photoelectrocatalysis, such as ZnO, $WO_3$ and $Fe_2O_3$.

Prakasam and colleagues [69] prepared nanoporous film of $Fe_2O_3$ by submitting a Fe foil to electrochemical anodization in electrolyte composed of 1% HF+0.5% ammonium fluoride +0.2% 0.1 M nitric acid ($HNO_3$) in glycerol (pH 3) at 10°C. LaTempa and colleagues [122] produced $\alpha$-$Fe_2O_3$ (hematite) nanotubes by potentiostatic anodization of iron foil in an ethylene glycol electrolyte containing $NH_4F$ and deionized water. Hematite has a band gap of ≈2.2 eV (indirect) and can absorb light at $\lambda \leq 560$ nm; it can therefore be activated in a large part of the solar spectrum.

Lai et al. [123] prepared $WO_3$ nanotubes by electrochemical anodization of W foil in electrolyte composed of 1 M of sodium sulphate+0.5 wt.% of ammonium fluoride at 40 V. The $WO_3$ is photoactive when irradiated by visible light due to its small band-gap energy (2.4 eV to 2.8 eV) and has attracted scientific interest in photo(electro)catalysis. Some reviews [29, 70] have explored the use of $WO_3$ photoanodes mainly in photoelectrochemical water splitting.

Park and colleagues [124] reported a synthesis of ZnO nanowires by electrochemical anodization on a Zn foil using as electrolyte 5 mM $KHCO_3$ aqueous solution. ZnO has a similar band gap and band positions of $TiO_2$ ($E_g$ about 3.2 eV), but higher quantum efficiency than $TiO_2$. On the other hand it has limited applications due to its photocorrosion in acidic medium [71].

## **4.2. Band-gap engineering**

Despite all the improvements made to $TiO_2$ as a photoactive catalyst, the material still presents problems, such as activation with UV irradiation ($\lambda$≤387 nm), due to its wide band gap ($E_g$=3.2 eV). Thus, the use of solar energy is limited since the activation of $TiO_2$ occurs only from UV light, which corresponds to a small fraction (≈5%) of the sun's energy compared to visible light (45%) [39]. In this sense, efforts have been directed at shifting the optical response of titanium dioxide from the UV to the visible spectral range, which would be of great utility in photo(electro)catalysis and other applications of $TiO_2$. This modification of optical properties of semiconductors has been called band-gap engineering [19, 39, 94, 107].

Modification of $TiO_2$ properties has been achieved mainly by (i) doping with different transition metal ions (such as Cr [125], Co [126], W [127], Zr [128] and Fe [129]) and with different anions (such as N [130], F [131], S [132], B [133], C [93]) that replace oxygen in the crystal lattice, and (ii) by surface decoration, which includes coupling with other semiconductors and deposition of particles of noble metals [14, 84, 134-137].

However, these arrangements frequently increase only the absorption and do not properly improve material properties such as the stability of the semiconductor under illumination, efficiency of the photocatalytic process, and the wavelength range response. One example is the CdS, which absorbs a good portion of the visible radiation but is usually unstable and photodegrades with time [138].

| Dopant/Modifier | Strategies | References |
|---|---|---|
| N | Anodization of Ti–N alloy*<br>Anodization in nitrogen-containing electrolyte*<br>Electrodeposition in nitrogen-containing electrolyte | [130], [139], [140], [141], [142], [143], [144], [145] |
| C | Anodization in carbon containing electrolyte* | [146], [147] |
| F | Anodization in containing electrolytes* | [143] |
| B | Anodization in boron-containing electrolyte*<br>Electrodeposition in boron-containing electrolyte | [133], [148], [149] [150] |
| W | Anodization of Ti–W alloy*<br>Anodization in tungsten-containing electrolyte* | [127], [151], [152] |
| Zr | Anodization in zirconium-containing electrolytes*<br>Electrodeposition in zirconium-containing electrolyte | [128], [153], [145] |
| La | Electrodeposition in lanthanum-containing electrolyte | [154] |
| Si | Anodization in silicon-containing electrolyte* | [152] |
| Nb | Anodization of Ti–Nb alloy* | [144] |
| Ag | Electrodeposition in silver-containing electrolyte | [155], [156] |
| Pt | Electrodeposition in platinum-containing electrolyte | [157], [158] |
| Pd | Electrodeposition in palladium-containing electrolyte | [159], [160] |
| CdS | Electrodeposition in Cd and S-containing electrolyte | [135], [161] |
| CdTe | Electrodeposition in Cd and Te-containing electrolyte | [162] |
| $Cu_2O$ | Electrodeposition in Cu-containing electrolyte | [163] |

*one-step synthesis

**Table 1.** Electrochemically doped/surface modified $TiO_2$ nanotube arrays

In order to make materials more photoactive under visible light and more stable under certain conditions, and to have lower band-gap energy, the doping of $TiO_2$ with several metals and non-metal compounds has also been explored: Table 1 shows a summary of the electrochemical methods adopted to promote doping/surface modification of $TiO_2$ nanotubes,with the related references.

### 4.2.1. Doped $TiO_2$ nanomaterials

Asahi et al. [164], in a 2001 study, developed a method for $TiO_2$ visible light activation through doping of C, N, F, P, or S for O in the anatase $TiO_2$ crystal using calculated densities of states (DOSs). They found that the substitutional doping of N was the most effective method because nitrogen p states contribute to band gap narrowing by mixing with O 2p states. Nitrogen can be easily introduced into the $TiO_2$ structure, due to its comparable atomic size with oxygen, small ionization energy and high stability.

There are two main ways to perform anion doping in $TiO_2$ by electrochemical techniques: (i) electrodeposition and (ii) adding a precursor of the element into the electrolyte during electrochemical anodization to oxide formation. It should be noted that for this the $TiO_2$ film must be immobilized on a conductive substrate, as in the case of $TiO_2$ NTs grown on metallic titanium.

In 2006, Shankar and colleagues [139] described a simple way to introduce N atoms into $TiO_2$. N-doped thin films were fabricated by anodic oxidation of a pure titanium sheet in electrolyte composed of 0.07 M HF, $NH_4NO_3$ (from 0.2 to 2.5 M) and $NH_4OH$ to adjust the pH to 3.5. The material showed optical absorption in the visible wavelength range from 400 to 530 nm. The XPS data confirmed that all the incorporated nitrogen is substitutional on the oxygen site, and the proportions of N atoms in $TiO_{2-x}N_x$ were x=0.23, x=0.09 and x=0.02. The N-doped samples exhibited a shift in absorption toward the visible spectra from 400 to 510 nm. Antony and colleagues [140] prepared N-doped $TiO_2$ NTs by anodizing Ti foils in ethylene glycol+$NH_4F$ +water mixture containing urea as a nitrogen source. They used various concentrations of urea and achieved different N concentrations in $TiO_2$ film, determined by X-ray photoelectron spectroscopy (XPS). There was nitrogen incorporation in $TiO_2$lattice mainly in substitutional form (substitution of $O_2^-$ ions by $N^{3-}$ ions). The doped samples showed visible light response, and the calculated optical band gaps were 3.27, 3.21, 2.75 and 2.77 eV for pristine $TiO_2$, $TiO_{1.85}N_{0.115}$, $TiO_{1.813}N_{0.14}$and $TiO_{1.84}N_{0.121}$, respectively. Zhou et al. [141] fabricated N-doped using the same methodology, via anodic oxidation of Ti in electrolyte composed of ammonium fluoride ($NH_4F$) and triethylamine ($C_6H_{15}N$). Nitrogen was successfully introduced into the $TiO_2$ lattice replacing oxygen atoms, and as a result there was a shift of $TiO_2$ band edge from 380 nm to 405 nm in N-doped $TiO_2$.

Kim et al. [142] produced N-doped $TiO_2$NTs by anodization of a high-purity TiN alloy with approximately 5 at.% of N in a glycerol+water (50:50 vol%)+0.27 M $NH_4F$ electrolyte. XPS data of the sample surfaces indicated 2–3 at.% of N atoms present as Ti–O–N in the nanotubes. They found that the nanostructured layer grown on TiN alloy showed decreased UV response compared with pure $TiO_2$ NTs film, but showed a strongly increased photoresponse in visible light spectra.

Li and colleagues [165] used an electrochemical technique to dope $TiO_2$ with nitrogen atoms, in two steps. N-doped $TiO_2$ NTs were prepared by electrochemical anodization in glycerol electrolyte, followed by electrochemical deposition in $NH_4Cl$ solution. The optimal conditions in electrodeposition were: voltage of 3 V, reaction time 2 h, and $NH_4Cl$ concentration of 0.5 M. Both the photoelectrochemical properties and photocatalytic activity under visible light irradiation were enhanced after N doping into $TiO_2$ nanotube arrays.

By using the aforementioned electrochemical techniques for the nitrogen, it is also possible to perform doping with other non-metals, such as C and B, for example. Milad and colleagues [146] achieved carbon-doped titanium oxide nanotubular arrays via anodic oxidation of titanium foil at 20 V in acidic (0.5 M $H_3PO_4$+0.14 M NaF) and organic media (ethylene glycol +0.3 wt% $NH_4F$) with 0.5 and 1 wt% carbon source (polyvinyl alcohol). Approximately 2.75% and 8.45% carbon was incorporated into the TNT in the acidic and organic electrolyte, respectively. The highest photocurrent density was observed for the sample with the higher amount of carbon atoms incorporated. Krengvirat et al. [147] produced carbon-incorporated $TiO_2$ by anodic oxidation in EG containing 0.5 wt% $NH_4F$+1 wt% water. The interstitial carbon arising from the pyrogenation of ethylene glycol electrolytes induced a new C *2p* occupied state at the bottom of the $TiO_2$ conduction band, decreasing band-gap energy to 2.3 eV and consequently making the material visible-light active. Lu and colleagues [133] fabricated boron-doped $TiO_2$ NTs by electrochemical anodization in an electrolyte containing different concentrations of $NaBF_4$ as a boron source. XPS data showed that the boron atoms were incorporated into the $TiO_2$ lattice, forming a Ti–B–O bond. All the samples presented red shift (photoresponse under visible light) and higher photocurrents under visible light than the bare $TiO_2$ NTs. Li and colleagues [148] fabricated $TiO_2$ NTs by electrochemical anodization of Ti in 1 M $(NH_4)_2SO_4$ + 0.5 wt% $NH_4F$ electrolyte, and accomplished boron doping by electrodeposition in 0.1 M $H_3BO_3$ electrolyte (using current densities of 10 $\mu A/cm^2$ for 27 min). Using XPS data, B atoms were incorporated into $TiO_2$ matrix, and the B-doped samples exhibited red shift in absorption (380–510 nm) due to the excitation of electrons from the impurity energy levels located above the valence-band edge (provided by the B atoms), to the conduction band edge. The proposed mechanism is consistent with those reported for doping with carbon and nitrogen.

Besides anion doping, there are numerous papers that investigate the effect of doping with metal ions in the $TiO_2$ lattice. The metal ions can occupy two different positions in the $TiO_2$ matrix, which are substitutional and interstitial, depending on the ionic radius of the metal. The dopant occupies the interstitial sites if the dopant radius is much smaller than the matrix cation, in this case, titanium. If the dopant has similar ionic radius of Ti, the substitutional mode is adopted [7]. In metal-doped $TiO_2$, new energy states can be formed either within or beyond the VB and CB, decreasing band-gap energy. However, transition metals may also act as recombination sites and may cause thermal instability in the anatase phase of $TiO_2$ [7, 27].

Tungsten-doped $TiO_2$ NTs were prepared by Gong et al. [127] in glycerol/fluoride electrolyte containing sodium tungstate via the electrochemical oxidation of a Ti substrate. XPS data showed that the $W^{6+}$ ions were loaded into $TiO_2$ lattice by displacing $Ti^{4+}$ ions and forming W–O–Ti bonding. Thus, the UV−Vis spectra of W-doped samples show red shift and decrease the band-gap energy from 3.18 eV (bare $TiO_2$ NTs) to 2.97 eV (W-doped $TiO_2$ NTs). These findings can be attributed to the fact that the conduction band of the W-doped samples was reformed in the presence of $W^{6+}$ ions. Das and colleagues [151] prepared tungsten-doped $TiO_2$ NTs by electrochemical anodization of Ti–W alloys. The sample containing 9% W presented band-gap energy of 2.83 eV and higher visible photocurrents than undoped samples.

Liu and colleagues [153] produced Zr-doped $TiO_2$ NTs. They prepared $TiO_2$ NTs by electrochemical anodization in 0.14 M NaF and 0.5 M $H_3PO_4$ electrolyte, and made the zirconium doping by electrodeposition in 0.1 M $Zr(NO_3)_4$ electrolyte, varying the applied potential. When the amount of zirconium in $TiO_2$ was small (lower potentials of deposition) zirconium entered into the lattice of $TiO_2$, acting as defect positions, improving separation of charges. At higher Zr amounts, zirconium atoms were partially unable to enter into the $TiO_2$ lattice, acting as recombination sites on the $TiO_2$ surface, decreasing the photocatalytic efficiency. Using a similar approach, Nie and colleagues [154] produced lanthanum-doped (La-doped) $TiO_2$ NTs. After the preparation of $TiO_2$ NTs, they executed a cathodic electrochemical process using lanthanum nitrate solution as the La source. The material became visible photoactive, and the band gap was decreased from 3.32 eV (undoped) to 3.03 eV (La-doped NTs).

Another approach reported in the literature focuses on the incorporation of more than one anion (or an anion and a cation) in the structure of $TiO_2$, which is called codoping. Su et al. [143] prepared N-F-codoped $TiO_2$ NTs by electrochemical anodization of Ti in oxalic acid $+NH_4F$ electrolyte. N-doping into $TiO_2$ resulted in the creation of surface oxygen vacancies, and F-doping produced several beneficial effects, such as the creation of surface oxygen vacancies, which enhance the surface acidity, and creation of $Ti^{3+}$ ions, which reduce electron/hole recombination. Zhou and colleagues [149] produced B,N-codoped $TiO_2$ nanotube arrays. Sun et al. [152] produced Si–W codoped $TiO_2$ NTs using a one-step anodization process with the presence of silicotungstic acid in the electrolyte, and the doped samples presented visible photocurrent 2.5 times larger than bare $TiO_2$ NTs. Xua and colleagues [144] produced passivated n–p co-doping of niobium and nitrogen into $TiO_2$ lattice by anodizing Ti–Nb alloys and posterior N-doping. Liu et al. [145] produced N/Zr-codoped $TiO_2$nanotube arrays in a two-step process. Firstly they prepared the $TiO_2$ NTs by electrochemical anodization and then accomplished doping using electrochemical deposition in $Zr(NO_3)_4$ and $NH_4Cl$ electrolyte. The doped materials presented increased photoactivity under UV and visible light; the visible light sensitivity was caused by N-doping, and Zr-doping was responsible for enhancing the charge separation.

Although several mechanisms have been proposed for doping from experimental and theoretical data, it is not possible to clearly understand the role of dopants and therefore there is no consensus in the scientific community [7, 166]. Table 1 shows a summary of the electrochemical strategies fordopingTiO$_2$ nanotubes, with the related references.

### *4.2.2. Composite semiconductor as photocatalysts*

The coupling of two semiconductors with appropriate energy CB and CV can reduce the recombination of $e^-/h^+$ pairs due to the transfer of carriers from one semiconductor to the other, as can be seen in Figure 8. Furthermore, depending on the band-gap energy of the semiconductor used, the composite can be activated in the visible region [7].

There are few papers that report on the coupling of semiconductors by electrochemical techniques. In this case, the composite is produced by a two-step process. CdS is the most used semiconductor to coupling with $TiO_2$ due to its small band-gap energy ($E_g$=2.4 eV). Li and colleagues [135] produced CdS nanoparticles-modified $TiO_2$ nanotube arrays by electrodeposition via direct current. In the electrodeposition step, they used as electrolyte a mixed solution of 0.01 M $CdCl_2$ in dimethyl sulphoxide (DMSO) with saturated elemental sulphur. CdS was cathodically electrodeposited at the optimum constant DC density of 0.5 mA $cm^{-2}$ for 5–15 min. They found that the photocurrents of CdS/$TiO_2$ NTs were much larger than those of pure $TiO_2$ NTs. Under UV−Vis irradiation, both semiconductors are excited and as the conduction band of $TiO_2$ is more anodic than that of the CdS there is efficient electron transfer between the CdS and $TiO_2$. Thus, the photogenerated electrons are injected from the conduction band (CB) of CdS to the CB of $TiO_2$; at the same time, the holes transfer from the valence band (VB) of $TiO_2$ to the VB of CdS. In heterojunctions such as CdS/$TiO_2$ there are less electron/hole recombinations and enhanced light absorption, both UV and visible. Zhang et al. [161] prepared water-soluble CdS quantum dots (QDs) and deposited on highly ordered $TiO_2$NTs by various methods, including cyclic voltammetric (CV) electrodeposition. The QDs were prepared using 0.01 mol $L^{-1}$ cadmium nitrate and 0.01 mol $L^{-1}$ sodium sulphide dissolved in 6 × $10^{-5}$ mol $L^{-1}$ *N*-cetyl-*N*,*N*,*N*-trimethyl ammonium bromide aqueous solution. The CV electrodeposition was carried out in a conventional three-electrode system with $TiO_2$ NTs as the working electrode under applied voltage sweeps from −0.8 to 0.2 V versus SCE and a scan rate of 30 mV $s^{-1}$. The yielding composites of CdS/$TiO_2$ NTs prepared by CV showed excellent photoelectrical behaviour and superior visible-light photocatalytic activity due to the solid binding and effective coupling between the QDs and the $TiO_2$ NTs.

Feng and colleagues [162] prepared a heterojunction of CdTe/$TiO_2$ NTs. CdTe is a direct band-gap semiconductor with $E_g$=1.5 eV, absorbing almost across the visible spectrum. After the preparation of $TiO_2$ NTs, CdTe nanoparticles were pulse electrodeposited in a conventional three-electrode system (with the $TiO_2$ NTs as working electrode) in electrolyte solution containing 0.08 mol $L^{-1}$ $CdSO_4$ and 0.05 mol $L^{-1}$ $NaTeO_3$. The pulse on–off time ratio was 0.2:1, with a running voltage of −1 V. A red shift of 50 nm was observed in CdS/$TiO_2$ NTs composite and the calculated optical band gap was 1.5 eV. The positions of CB and VB in relation to the $TiO_2$were similar to the CdS; there was electron injection from the photoexcited CdTe to $TiO_2$ CB, and the photogenerated holes moved from the $TiO_2$ VB to the CdTe VB, preventing the recombination of charges.

Tsui and colleagues [163] studied the modification of $TiO_2$ NTs with $Cu_2O$ by electrodeposition. $Cu_2O$ is a p-type semiconductor with a direct band gap of 1.95–2.2 eV. The junction between p-type $Cu_2O$ and n-type $TiO_2$ in principle enhances the separation of electron/hole pairs; the $Cu_2O$ is also visible-light responsive. Electrodeposition of $Cu_2O$ was performed using the as-prepared $TiO_2$ NTs with working electrode using a three-step pulse plating method (−0.5 V for 5 ms, −0.3 V for 0.5 ms, and 0 V for 5 s) from a solution containing 0.02 M $Cu(CH_3COO)_2$ and 0.1 M $NaCH_3COO$ (pH 5.7). The $Cu_2O$/$TiO_2$ composite presented visible light absorption and

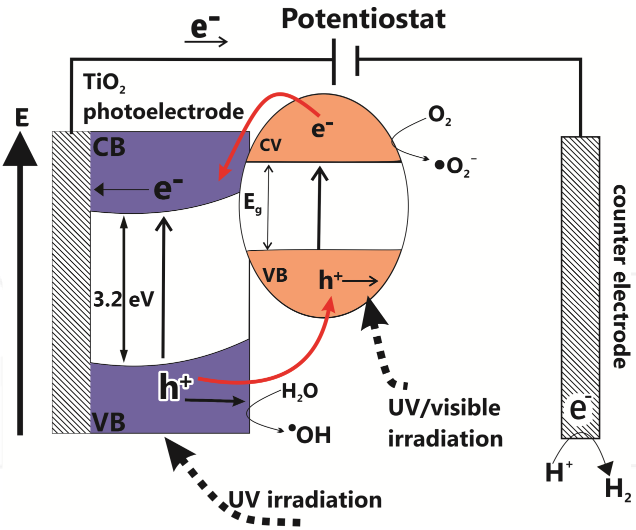

**Figure 8.** Schematic representation of the mechanism of charges separation in a photoelectrochemical system operatedby coupling a visible active semiconductor to a $TiO_2$ electrode

the band gap values obtained were 3.27 eV for $TiO_2$ and 2.21 eV for $Cu_2O/TiO_2$ heterojunction. However, $Cu_2O$ on $TiO_2$ NTs dissolves under intense light, limiting the use of $Cu_2O$ in photoelectrochemical devices.

### *4.2.3. Metal deposition*

The decoration of $TiO_2$ by dopants of nanoparticles of noble metals (such as Ag, Au, Pt, and Pd) has attracted attention in order to enhance the photoactivity of the material. Due to different Fermi levels of $TiO_2$ and the metal nanoparticles, a Schottky barrier can be formed in the new material. Therefore, there is a rectification of the charge carrier transfer where the energetic difference at the semiconductor/metal interface drives the $e^-$ from the CB of the $TiO_2$ into the metal nanoparticles. In other words, the metal acts as an electron trap, promoting interfacial charge transfer and therefore minimizing recombination of the $e^-/h^+$ pairs, as shown in Figure 9 [7].

Xie and colleagues [155] produced Ag-loaded $TiO_2$ NTs using pulse current deposition technique in 0.01 M $AgNO_3$ and 0.1 M $NaNO_3$ electrolyte, using the as-prepared $TiO_2$ NTs as working electrode. They applied $-15$ mA $cm^{-2}$ of pulse current with 0.1 s on-time and 0.3 s off-time. Highly dispersed Ag nanoparticles of 10–40 nm were deposited on $TiO_2$. $TiO_2$ NTs and $Ag/TiO_2$ NTs showed a similar maximum photocurrent density $\lambda$ ($i_{max}$ 330 nm), but $Ag/TiO_2$ NTs displayed much more intensive photocurrent response, which can be explained by the Schottky barrier formation separating the charge carriers more efficiently. Zhang and colleagues [156] prepared N-doped $TiO_2$ NTs and loaded Ag nanoparticles on the $TiO_2$ surface by

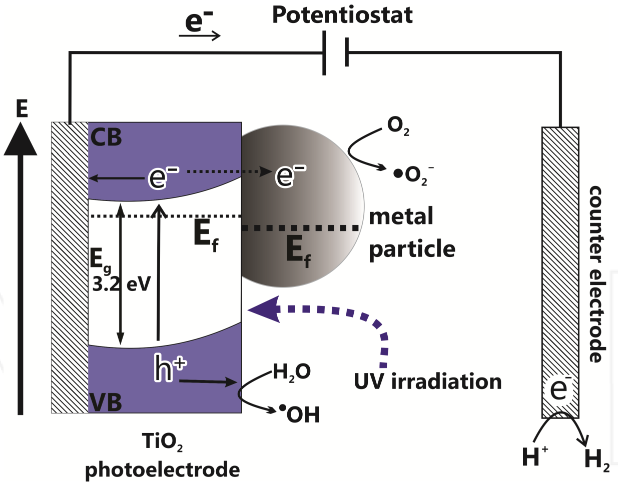

**Figure 9.** Metal coupling on $TiO_2$ surface and the mechanism of charge separation in a photoelectrochemical system

electrochemical deposition using 0.2 g $L^{-1}$ $AgNO_3$ in 2.5 g $L^{-1}$ EDTA solution applying −0.1 V for 1−20 s.

Xing et al. [157] produced Pt-nanoparticles-decorated $TiO_2$ NTs by cyclic voltammetry electrodeposition in 19.3 mM $H_2PtCl_6$ solution from −0.4 to 0.5 V at a scan rate of 10 mV $s^{-1}$ (controlling the number of cycles). Yin and colleagues [158] also prepared Pt/$TiO_2$ NTs using an electrochemical approach, but using AC electrodeposition at 2–4 V for 5–30 min in solution containing 1 mmol $L^{-1}$ of $H_2PtCl_6$.

In the paper of Qin and colleagues [159] Pd particles were deposited onto the $TiO_2$ NTs electrode by a pulse electrodeposition technique in $PdCl_2$ (2 g $L^{-1}$) electrolyte solution (pH 1.5). Cheng et al. [160] prepared Pd/$TiO_2$ NTs through an electrochemical deposition method at a constant potential of −0.8 V using $PdCl_2$ solution (1 mM) in 0.5 mol $L^{-1}$ NaCl electrolyte. The Pd/TNTs sample displayed absorption between 540 nm and 700 nm and presented transient photocurrent density of about 0.094 mA $cm^{-2}$, higher than that of TNTs (0.067 mA $m^{-2}$) under xenon lamp irradiation, indicating that decoration with Pd improves the charge separation, according to the Schottky barrier formation mechanism.

All these materials have been demonstrated to massively improve photoelectrocatalytic oxidation processes. Works dealing with water contaminated by a wide range of compounds are discussed below and summarized in Table 2.

## 5. Application of nanostructured materials in photoelectrocatalysis

As the complexity of contaminants increases, the efficiency of photoelectrocatalytic treatment methods needs to be enhanced by the use of different strategies, as they pose a potential risk to the environment. Most reported work tackles the oxidation of organic pollutants, such as dyes of different classes and industry uses, hormones, pharmaceuticals, pesticides, etc. Oxidation of biological microorganisms such as bacteria and fungus has also been investigated. In all these studies, oxidation is promoted by $^{\bullet}OH$ action generated at the interface photoanode/electrolyte. As discussed previously, these hydroxyl radicals are generated on n-type semiconductors when the holes ($h^+$) on the electrode surface react with water and/or hydroxyl ions.

The reduction of inorganic contaminants has been studied as well. The main contaminants described have been bromide, nitrate, nitrite and $CO_2$. In this case, the reduction takes place at a p-type semiconductor [12]. The reduction of toxic metals ($Cr^{6+}$ to $Cr^{3+}$) has also been described [61] in a photoelectrocatalytic process where the cathode is Pt but is conjugated in a system where the organic molecules are oxidized simultaneously in a photocathode such as $Ti/TiO_2$ and the electrons are forwarded to the counter electrode, where the reduction of Cr (VI) takes place [167]. Solar conversion of $CO_2$ to hydrocarbon fuels seems promising to reduce global warming for improved sustainability. Solar fuels include hydrogen, carbon monoxide, methane and methanol [168].

More recently, the application of semiconductor materials has received a great deal of attention in a re-emerging field: the generation of hydrogen as a clean energy carrier. Studies have described the direct water splitting process and the degradation of organic pollutants in order to obtain hydrogen [16]. For this purpose, the use of n and p-type semiconductor materials using the photoelectrocatalysis method was investigated. The choice of the semiconductor material for hydrogen generation purposes depends on the valence and conduction-band energy levels, which are pH dependent (Figure 10).

The lower edge of the conduction band needs to be greater than the energy level for $H_2$ evolution (according to Equation 11). For water-splitting purposes (Figure 10), the upper edge of the valence band needs to have enough energy to promote the $H_2O/O_2$ reaction (Equation 12), while for simultaneous organic-pollutant removal the energy level must be more electropositive than the $OH^-/^{\bullet}OH$ level for hydroxyl radical formation (Equations 11,12):

$$2H^+ + 2e^- \rightarrow H_2 \tag{11}$$

$$2H_2O \rightarrow O_2 + 4e^- + 4H^+ \tag{12}$$

The use of solar light for hydrogen generation purposes has been desirable for the same reasons as for PEC purposes. Hence, the development of photoanodes that absorb light in the visible region ($\lambda$>400 nm) is necessary, and could be achieved by lowering the photoanode band-gap energy.

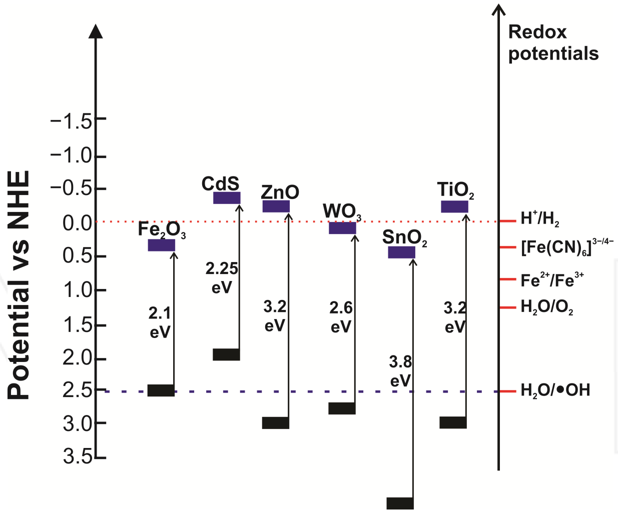

**Figure 10.** Schematic representation of $E_g$ values (in eV) and position of CB and VB for the main semiconductors

### 5.1. $TiO_2$ nanomaterials applied to water treatment

The use of $TiO_2$-nanostructured materials in the removal of contaminants is undoubtedly a successful system in the treatment of wastewater. The use of nanotubes obtained from different routes has been described as an efficient alternative method to promote higher discoloration and partial mineralization of main organic pollutants, as they have a high and homogenous surface area and suitable photocurrent values.

The degradation of organochlorinated compounds [169, 170], pesticides [171, 172], aromatic amines [10], biological microorganisms [14, 15], hormones (endocrine disrupters) [173, 174], flameretardants [175] and mainly dyes [176] has been reported with high efficiency shown by nanotube materials acting as photoanodes in photoelectrocatalytic treatment.

$TiO_2$ NTs have proved to be more photoactive and to improve the efficiency of PEC degradation of pentachlorophenol under biased potential, with sodium sulphate as electrolyte (0.01 mol $L^{-1}$) and low pH of the original solution. The photoelectrocatalytic processes have been shown to be more efficient than electrocatalytic, photolytic and photocatalytic techniques [169]. Quan and colleagues [170] also observed the synergistic effect of photoelectrocatalysis compared to photocatalytic and electrochemical processes aiming at the degradation of pentachlorophenol in aqueous solution. They also reported that $TiO_2$ NTs under UV irradiation promoted higher mineralization than a conventional sol-gel film electrode.

The photoelectrocatalytic degradation of pesticides has been performed by $TiO_2$ thin films. Philippidis and colleagues achieved 82% of degradation of the pharmaceutical compound imidacloprid using Ti/$TiO_2$ electrodes prepared by the immobilization of P25 powder onto Ti substrate. The degradation efficiency increased with increased applied potential, following the first-order kinetics model after three hours of treatment. The method was proved to be more efficient than photocatalysis (63% removal) and photolysis (5% removal) operating under UV irradiation [171]. The pesticide Dipterex has been removed by using $TiO_2$ as a photoanode, prepared by a sol-gel method depositing over a nickel net. The method promoted a chemical oxygen demand (COD) removal and organophosphorous conversion of up to 82.6% and 83.5%, respectively, after 2 h of treatment under UV light [172].

The incomplete reduction of azo dyes and nitroaromatic compounds can usually promote aromatic amine formation, which can be released into the environment as potential carcinogens. This has been reported in drinking water treatment plants [177]. The use of $TiO_2$ NTs as photoanodes was proposed by Cardoso and colleagues. The method is efficient since it promotes the complete degradation and mineralization of 4,4-oxydianiline after 2 h of photoelectrocatalytic treatment under UV irradiation [10].

The PEC degradation of 4,4‘-dibromobiphenyl used in flame retardants in the textile, and electronic industries, and in additives in plastics, has been performed using $TiO_2$ NTs as photoanodes. This class of compounds is described as toxic to human health and the environment. The photoelectrocatalytic process was more efficient than the photocatalytic and electrolytic process alone. Different anodes were compared: $TiO_2$, $Zr/TiO_2$ and $Zr,N/TiO_2$ NTs. The photoelectrocatalytic efficiency was significantly affected by the properties of the catalysts and the best performance was observed with $TiO_2$ doped with nitrogen and zirconium, as it had a higher photocurrent under UV irradiation by a 125 W mercury lamp [175].

Biological microorganisms can cause the contamination of water by spreading potential pathogens. $TiO_2$ nanotube arrays and Ag-loaded $TiO_2$ NTs have been employed in the disinfection of water containing *Mycobacterium smegmatis*. Under UV irradiation the photoelectrochemical treatment promoted 100% inactivation after 3 min. The effect of Ag on $TiO_2$ NTs has been observed in TOC removal, which reached 98% and 90% for $Ag/TiO_2$ and $TiO_2$, respectively, after 4 h of treatment [14]. The inactivation of *Mycobacterium kansasii* and *Mycobacterium avium* has also been conducted on $TiO_2$ and $Ag/TiO_2$ NTs electrodes by photoelectrocatalytic oxidation. The inactivation of both bacteriawas 100% after 3−5 minutes of treatment, faster than photocatalytic and photolytic treatment methods, indicating that the bias potential of the photoanode potentializes the treatment [15]. Egerton and colleagues described the PEC inactivation of wastewater containing *E. Coli* using $TiO_2$ irradiated by UV light. The method is also efficient for the removal of 4-nitrophenol and humic acid contaminants [178].

Endocrine disrupters have been reported as a class of compounds which can mimic or inhibit the natural actions of the endocrine system in animals and humans, such as synthesis, secretion, transport and binding. They can be either natural or synthetic compounds that come from different sources, such as pharmaceutical compounds, personal care products, disinfectionproducts and surfactants [173]. The literature [11] reports the removal of Bisphenol A from wastewater using $TiO_2$ NTs in a photoelectrocatalytic oxidation process under UV light and applied potential of +1.2 V. The removal was confirmed by HPLC/DAD analysis. The degradation of carbamazepine has been conducted with $Ti/TiO_2$ electrodes prepared by pulsed laser deposition. After 120 min of treatment, 73.5% pollutant removal was achieved, and 21.2% mineralization. Although complete degradation was not achieved the by-products were not toxic in the presence of *Vibrio Fisheri* [174]. The removal of these compounds is better than that achieved by other methods, such as photocatalysis [179], activated sludge [180] and biological treatment [181].

Different activities in the textile, paper, pharmaceutical, leather and food industries, among others, release a huge amount of dyes in effluents that can reach drinking water treatment plants if they are not appropriately treated. There are serious concerns over these compounds – many are potential carcinogens, or have xenobiotic or toxic properties that can harm the environment and living organisms [176].

The PEC oxidation of methyl orange [182], methylene blue [183] and rhodamine B [184] dyes has been reported. The photoelectrochemical method promoted 100% discoloration and high reduction of the toxicity of dispersed and indigoid organic dyes [185-187].

Recently, the main target of PEC studies has been the visible light activation of materials [188]. The relevance of reactors for photoelectrocatalytic treatment has also been described. It has been mentioned that the use of solar cells to supply the energy in PEC systems could reduce the cost of batch reactors by making it unnecessary to purchase electricity –electricity costshave been pointed out as the main disadvantage of this process [189].

For hydrogen production, a lot of photocatalysts have been studied in the literature,though mainly $TiO_2$ and modified $TiO_2$. Lianos described the use of $TiO_2$ supported on ITO and FTO and $TiO_2$ doped with N, C and S as well as the use of photocatalysts combined with noble metals such as Pt, Pd and Au and the coupled semiconductors $TiO_2/SnO_2$, $TiO_2/WO_3$, $TiO_2/RuO_2$, $TiO_2/V_2O_5$ in an attempt to use visible light irradiation [16]. Pure $TiO_2$ nanotube arrays have also been described in photoelectrochemical water splitting and simultaneous degradation of methylene blue [78]. The PEC experiments were conducted using an artificial sunlight simulator. The higher photoconversion efficiency for hydrogen generation and the degradation efficiency of MB were attributed to the better electron transfer process observed for two-step $TiO_2$ NTs over one-step $TiO_2$ NTs. $CdS/TiO_2$ nanotubes for photoelectrochemical hydrogen production have also been described: the doped material presented a better performance in the $H_2$ generation rate than the pure $TiO_2$ NTs under solar light illumination [190].

Zhao and colleagues carried out simultaneous photoelectrochemical destruction. They obtained contaminant and nickel recovery on the cathode. The deposition of $TiO_2$ film was performed by dip-coating [167]. Paschoal and colleagues promoted the photoelectrochemical reduction of bromate under $Ti/TiO_2$ coated as a photocathode. Photoelectrocatalytic reduction of $BrO_3^-$ to $Br^-$ can reach 70% at neutral pH under biased potential of −0.20 V after 75 minutes of treatment [191]. Table2 shows a summary of the selected studiesusingdopedand undoped $TiO_2$ photoanodes used in photoelectrocatalytic applications.

| Photoanode | PEC application | Reference |
|---|---|---|
| $TiO_2$ NTs | Organics degradation | [10], [169], [170], [11], [192], [175], [193] |
| | Water splitting | [194, 195], [196], [197] |
| $TiO_2$ NTs coupled with other semiconductors | Organics degradation | [9], [198], [199], [200], [186], [201], [162] |
| | Water splitting | [202] |
| Anion-doped $TiO_2$ NTs | Organics degradation | [203], [143], [133], [148], [149] |
| | Water splitting | [204], [147], [93] |
| Cation-doped $TiO_2$ NTs | Organics degradation | [127], [154], [205] |
| | Water splitting | [128] |
| $TiO_2$ NTs coupled with noble metals | Organics degradation | [206], [207] |
| | Water splitting | [208], [158] |
| | Disinfection | [14], [15], [209] |
| $TiO_2$ thin film | Organics degradation | [171], [172], [189] |
| | Water splitting | [210], [211] |
| | Disinfection | [212], [62] |
| Doped $TiO_2$ thin film | Organics degradation | [213], [214], [215], [205], [216] |

**Table 2.** Photoelectrocatalytic applications of doped and undoped $TiO_2$-based nanostructured semiconductors

### 5.2. Application of doped, decorated and composite of $TiO_2$ nanomaterials PEC

N-doped $TiO_2$ coatings prepared by radiofrequency magnetron sputtering has been employed on the degradation of the antibiotic chlortetracycline under 0.6 A of current intensity and solar simulator irradiation during 180 min, leading to 99% degradation. This is more efficient than pure Ti/$TiO_2$. This process has also shown to be efficient in the inactivation of faecal coliform, which is an indicator pathogen [217]. Wu and Zhang [204] prepared nitrogen-doped double-wall $TiO_2$ NTs, which under simulated solar light presented a high photoelectrochemical water splitting performance due to the high surface areas and absorbance in the visible light region. Sun et al. [203] prepared N-doped $TiO_2$ NTs, which presented better efficiency in Rhodamine B PEC degradation.

Boron-doped $TiO_2$ NTs have also been studied as photoanodes prepared by chemical vapour deposition. The electrode was applied in the degradation of methyl orange dye under visible light irradiation promoting 100% discoloration under applied potential of +2.0 V and UV irradiation [192]. In the studies by Lu and colleagues [133] and Li et al. [148] boron-doped $TiO_2$ NTs were prepared and applied in the PEC degradation of atrazine and phenol, respectively.

$TiO_2$ has been doped with nickel and used as a photocatalyst in the degradation of Acid Red 88 dye. The photoanode powder was prepared by the sol-gel method and 95% COD and TOC removal was obtained after 35 min of treatment under UV and solar irradiation. The colour removal was 72% for photocatalytic treatment and 97% for photoelectrocatalytic treatment under +1.6 V [189]. Gong and colleagues prepared W-doped $TiO_2$ NTs and applied these in simultaneous Rhodamine B degradation and production of hydrogen [127]; tungsten-doped $TiO_2$ films were also applied in dodecyl-benzenesulfonate removal by PEC [213].

Arrays of porous iron-doped $TiO_2$ as photoelectrocatalyst with controllable pore size have been synthesized by using polystyrene spheres as templates. It was found that photoelectrochemical hydrogen generation was favoured by a shift in the flat-band potential from −0.38V to −0.55 V vs. SCE and an increase of photocurrent by 80% [218].

Pt-deposited $TiO_2$ photoanodes have been prepared by a sol-gel method, where the amount of Pt was shown to interfere with the photoelectrochemical response for glucose oxidation. The increased Pt lowered the photocurrent but the overall oxidation efficiency of the PEC process was better than the PC process, for both $TiO_2$ and Pt-$TiO_2$ films [219]. Ye et al. [208] prepared $TiO_2$ NTs sensitized by palladium quantum dots (Pd QDs), which exhibit highly efficient photoelectrocatalytic hydrogen generation. Zhang and colleagues [206] prepared $TiO_2$ NTs loaded with Pd nanoparticles, and the PEC activity was investigated with degradation of methylene blue and Rhodamine B.

CdS-ZnS/$TiO_2$ composite material has been investigated in the production of electricity. The band-gap energy can be tuned between that of ZnS (3.5 eV) and that of CdS (2.3 eV) by varying Cd (or Zn) content. Photocatalytic and photoelectrocatalytic processes in basic electrolyte with ethanol as a sacrificial electron donor was also investigated. The performance of CdS-ZnS, Pt/(CdS-ZnS), Pt/(CdS-ZnS)/$TiO_2$ and Pt/$TiO_2$ photoanodes was compared and 75% CdS–25% ZnS over pure $TiO_2$ presented better electrocatalyst effect than 100% CdS over $TiO_2$ [220]. CdS nanocrystallites-decorated $TiO_2$ nanotube array photoelectrodes were prepared through anodization and electrodeposition strategies. Enhancement of photoelectrocatalytic degradation of Rhodamine B was achieved under Xenon light irradiation [198].

Georgieva and colleagues described the use of bicomponent anodes of $TiO_2$/$WO_3$ for the photoelectrocatalytic oxidation of organic species. $WO_3$ is a promising additive for $TiO_2$ since it modifies its photochemical properties in a favourable manner, both with respect to reduced recombination and visible light activity because of the lower band-gap energy. The coupling of semiconductor oxides leads to electron and hole transfer between the two materials in opposite directions, thus limiting recombination of the photogenerated species in the same material [29]. These materials have been employed in the degradation of 2,3-dichlorophenol under visible light irradiation [199], the removal of the hair dye Basic Red 51 under UV and visible light source [200] and the PEC oxidation of indigo carmine dye [186].

The use of heterojunctions was studied by Christensen and colleagues, who conducted the PEC degradation of *E. Coli* under UV irradiation using Si/$TiO_2$/Au as photoanode. The experiments were performed in water and air [221]. The silicon nanowire/$TiO_2$ heterojunction arrays were employed on the PEC degradation of phenol under simulated solar light irradiation. The kinetic constant and total organic carbon (TOC) removal were 1.7 times and two times as great as those of n-Si/$TiO_2$, respectively [222].

The PEC degradation of flame-retardants has been described under macroporous silicon/ graphene (MPSi/Gr) heterostructure. The experiments were conducted under visible light irradiation and compared to photocatalytic degradation. The photoelectrocatalytic degradation five times faster than PC degradation [223].

CdTe nanotubes have been produced by using ZnO as a template on an ITO surface. These were then used with the photoelectrocatalytic degradation of the Acid Blue 80 dye. This study provided a good strategy for the design of visible light-responsive photocatalysts that can be recycled and possess high efficiency, extremely low mass and high chemical stability [224].

The PEC remediation of 2,4-dichlorophenol by visible-light-enhanced $WO_3$ has also been described. The degradation process achieved 74% pollutant removal after a period of 24 hours, monitored by both chemical analysis and a bacterial biosensor (*Escherichia coli*) toxicity assay [225].

For hydrogen production, photocatalysts reported in the literature apart from $TiO_2$ include ZnO, $Fe_2O_3$, and $SrTiO_3$, which has the energy levels necessary to create active radical species that could efficiently carry out photodegradation process [16]. Under visible light irradiation some n-type materials have been described: nanoporous $WO_3$, $\alpha$-$Fe_2O_3$ or haematite and nanocrystalline $BiVO_4$ [18].

The Cu/$Cu_2O$ system as photocathode has been described in relation to nitrate removal under UV irradiation and biased potential. The material was prepared by electrodeposition and long-term stability was achieved. 93% nitrate removal was achieved after 75 min under the best experimental conditions. Nitrate reduction on Cu/$Cu_2O$ photoelectrodes occurs in the cathodic compartment cell via electrons generated under UV irradiation, as expected for a p-type electrode, leading to 42% of remaining nitrite and 52% gaseous nitrogen derived, respectively [12].

Zanoni and colleagues employed $TiO_2$ NTs in the photoelectrocatalytic oxidation of an organic synthetic dye (reactive black 5) and the simultaneous hydrogen generation. The photoanode was irradiated with UV light and biased at +1.0 V. Complete dye degradation and 72% mineralization was achieved after 2 h of treatment. The estimated overall hydrogen generation was around 44%, which corresponds to 0.6 mL $cm^{-2}$ [226].

## 6. Final remarks

Photoelectrocatalysis is an emerging field with many applications, such as organics oxidation, inorganics reduction, biological materials and production of electricity and hydrogen.

The technique could be described as a multidisciplinary field, where the basic concept is the irradiation by light ($h\nu \geq E_g$) of the semiconductor surface. There is the generation of electron/ hole pairs ($e^-/h^+$) by the promotion of an electron from the valence band (lower energy level) to the conduction band (higher energy level). The electrons are forwarded to the counter electrode under positive anodic bias (n-type) in order to minimize the recombination of these pairs due to the short life-time. When immersed in electrolyte the adsorbed water molecules and/or hydroxyl ions react with the holes on the valence band to generate hydroxyl radicals ($^\bullet OH$), which are a powerful oxidizing agent.

Titanium dioxide ($TiO_2$) is a classic example of an n-type semiconductor widely used as a catalyst for heterogeneous photocatalysis and photoelectrochemical applications. It has received a great deal of attention due to its good chemical and thermal stability, non-toxicity, low cost, high photoactivity and other advantageous properties. It is a typical n-type semiconductor mainly composed of anatase and rutile allotropic forms whose band-gap energy is 3.2 and 3.0 eV, respectively. The anatase phase is the desired form as it is more photoactive than the other forms.

The degradation of organic pollutants by photoelectrocatalysis has been described in the literature as one of the most effective treatments among advanced oxidative processes (AOPs) in the oxidation of recalcitrant compounds, as they are harmful to the environment and human health. The contamination of water is an increasing concern because pollutants can accumulate in the environment and are mutagenic and genotoxic.

The architecture of nanostructures used in the electrode construction has deeply influenced the results of PEC. Nanotube, nanowire, nanofibre, nanorod, and nanowall morphologies can be easily obtained by electrochemical methods. These kinds of nanostructures have improved efficiently organic contaminants degradation, especially due to their high surface area and ability to minimize charge recombination. The use of nanotube arrays has received a great deal of attention especially because it is the structure with the highest surface area/geometric area ratio; moreover, it is of a highly oriented and organized nature, leading to efficient charge transport as it has a unique and effective direct interfacial direction, decreasing the charge recombination effect. Among all $TiO_2$ NTs preparation routes, the electrochemical anodization method presents the greatest advantages, since they are cheaper, simpler and allow precise control of dimensions, presenting highly ordered nanotube arrays. The first generation of nanotube materials applied in PEC materials were obtained in aqueous solutions with the addition of $HNO_3$, $H_2SO_4$ and $H_3PO_4$ to HF acid as electrolyte. The second generation of nanotube arrays was obtained in buffered electrolytes. Aiming for better quality and performance, the third generation was obtained in organic medium as ethylene glycol, diethylene glycol, glycerol and $NH_4F$. Non-fluoride-based electrolytes are classified as the fourth generation, where HCl, $H_2O_2$ and a combination of both are used as electrolyte. Nanotube array photoanodes have presented good results on the water decontamination of organic contaminants and also water disinfection.

Recently, studies have addressed the challenge of obtaining PEC materials which can be activated by visible light, with the aim of using solar light to promote photoactivation, not only to reduce cost but also to establish an environmentally friendly method. For this purpose, different strategies are discussed in the literature to improve photoactivity and shift the PEC material absorption to the visible region, such as the use of photoanodes decorated with Ag and Pt, or combinations of semiconductors like $ZnO/TiO_2$, $CdS/TiO_2$, $WO_3/TiO_2$ in order to obtain composite and bicomponent materials; doping with metals (Fe, Mn, Cr), non-metals (B, C, Si) and co-doping (N-F, N-C) has also been thoroughly described.

Therefore, the use of $TiO_2$ and other materials is of huge relevance to photoelectrocatalysis applied to water treatment, and the success of photoanodes and photocathodes depends on the synthesis process and a better understanding of materials' properties.

## 7. Summary

The importance of photoelectrocatalysis has been discussed, with emphasis on recent advances in $TiO_2$-based materials and strategies of electrochemical synthesis and modification. Currently, $TiO_2$ nanotube arrays occupy a prominent position. These can be prepared by electrochemical anodization of titanium plates in fluoride-containing electrolytes. In the search for catalysts that can be photoactivated with visible radiation, doping or modification of these materials can be easily performed by electrochemical techniques. The use of these photocatalysts immobilized on conducting substrates employed in photoelectrochemical reactors is a viable strategy for increasing the efficiency of water splitting or to promote efficient degradation of organic compounds.

## Author details

Guilherme Garcia Bessegato, Thaís Tasso Guaraldo and Maria Valnice Boldrin Zanoni*

*Address all correspondence to: boldrinv@iq.unesp.br

Department of Analytical Chemistry, Institute of Chemistry, Universidade Estadual Paulista (Unesp), Araraquara, Brazil

## References

[1] Heller A. Conversion of sunlight into electrical power and photoassisted electrolysis of water in photoelectrochemical cells. Accounts of Chemical Research 1981; 14(5): 154-62.

[2] Tryk DA, Fujishima A, Honda K. Recent topics in photoelectrochemistry: achievements and future prospects. ElectrochimicaActa 2000; 45(15-16): 2363-76.

[3] Bard AJ. Photoelectrochemistry. Science 1980; 207(4427): 139-44.

[4] Daghrir R, Drogui P, Robert D. Photoelectrocatalytic technologies for environmental applications. Journal of Photochemistry and Photobiology A: Chemistry 2012; 238: 41-52.

[5] Linsebigler AL, Lu GQ, Yates JT. Photocatalysis on $TiO_2$ Surfaces-Principles, Mechanisms, and Selected Results. Chemical Reviews 1995; 95(3): 735-58.

[6] Kronik L, Shapira Y. Surface photovoltage phenomena: theory, experiment, and applications. Surface Science Reports 1999; 37(1-5): 1-206.

[7] Zhang H, Chen G, Bahnemann DW. Photoelectrocatalytic materials for environmental applications. Journal of Materials Chemistry 2009; 19(29): 5089-121.

[8] Fujishima A, Honda K. Electrochemical Photolysis of Water at a Semiconductor Electrode. 1972; 238(5358): 37-8.

[9] Bessegato GG, Cardoso JC, Silva BF, Zanoni MVB. Enhanced photoabsorption properties of composites of Ti/$TiO_2$ nanotubes decorated by $Sb_2S_3$ and improvement of degradation of hair dye. Journal of Photochemistry and Photobiology A: Chemistry 2013; 276: 96-103.

[10] Cardoso JC, Lizier TM, Boldrin Zanoni MV. Highly ordered $TiO_2$ nanotube arrays and photoelectrocatalytic oxidation of aromatic amine. Applied Catalysis B-Environmental 2010; 99(1-2): 96-102.

[11] Brugnera MF, Rajeshwar K, Cardoso JC, Boldrin Zanoni MV. Bisphenol A removal from wastewater using self-organized $TiO_2$nanotubular array electrodes. Chemosphere 2010; 78(5): 569-75.

[12] Monteiro Paschoal FM, Nunez L, de Vasconcelos Lanza MR, Boldrin Zanoni MV. Nitrate Removal on a Cu/$Cu_2O$ Photocathode under UV Irradiation and Bias Potential. Journal of Advanced Oxidation Technologies 2013; 16(1): 63-70.

[13] LaTempa TJ, Rani S, Bao N, Grimes CA. Generation of fuel from $CO_2$ saturated liquids using a p-Si nanowire parallel to n-$TiO_2$ nanotube array photoelectrochemical cell. Nanoscale 2012; 4(7): 2245-50.

[14] Brugnera MF, Miyata M, Zocolo GJ, Fujimura Leite CQ, Boldrin Zanoni MV. Inactivation and disposal of by-products from Mycobacterium smegmatis by photoelectrocatalytic oxidation using Ti/$TiO_2$-Ag nanotube electrodes.Electrochimica Acta 2012; 85: 33-41.

[15] Brugnera MF, Miyata M, Zocolo GJ, Fujimura Leite CQ, Boldrin Zanoni MV. A photoelectrocatalytic process that disinfects water contaminated with Mycobacterium kansasii and Mycobacterium avium. Water Research 2013; 47(17): 6596-605.

[16] Lianos P. Production of electricity and hydrogen by photocatalytic degradation of organic wastes in a photoelectrochemical cell: The concept of the Photofuelcell: A review of a re-emerging research field. Journal of Hazardous Materials 2011; 185(2-3): 575-90.

[17] Paulauskas IE, Katz JE, Jellison GE, Jr., Lewis NS, Boatner LA. Photoelectrochemical studies of semiconducting photoanodes for hydrogen production via water dissociation. Thin Solid Films 2008; 516(22): 8175-8.

[18] Abe R. Recent progress on photocatalytic and photoelectrochemical water splitting under visible light irradiation. Journal of Photochemistry and Photobiology C: Photochemistry Reviews 2010; 11(4): 179-209.

[19] Paramasivam I, Jha H, Liu N, Schmuki P. A Review of Photocatalysis using Self-organized $TiO_2$ Nanotubes and Other Ordered Oxide Nanostructures. Small 2012; 8(20): 3073-103.

[20] Roy P, Berger S, Schmuki P. $TiO_2$ Nanotubes: Synthesis and Applications. AngewandteChemie-International Edition 2011; 50(13): 2904-39.

[21] Andreozzi R, Caprio V, Insola A, Marotta R. Advanced oxidation processes (AOP) for water purification and recovery. Catalysis Today 1999; 53(1): 51-9.

[22] Pichat P, Disdier J, Hoang-Van C, Mas D, Goutailler G, Gaysse C. Purification/deodorization of indoor air and gaseous effluents by $TiO_2$ photocatalysis. Catalysis Today 2000; 63(2-4): 363-9.

[23] Villa RD, Trovo AG, Pupo Nogueira RF. Soil remediation using a coupled process: soil washing with surfactant followed by photo-Fenton oxidation. Journal of Hazardous Materials 2010; 174(1-3): 770-5.

[24] Rajeshwar K. Fundamentals of Semiconductor Electrochemistry and Photoelectrochemistry. In Licht S. (ed.) Semiconductor Electrodes and Photoelectrochemistry, Encyclopedia of Electrochemistry,Weinheim: Wiley 2007; 6: 1-51. Available at http://www.wiley-vch.de/bard/eoe/pdf/v06_1.pdf (accessed 15 November 2013).

[25] Rajeshwar K, Osugi ME, Chanmanee W, et al. Heterogeneous photocatalytic treatment of organic dyes in air and aqueous media. Journal of Photochemistry and Photobiology C: Photochemistry Reviews 2008; 9(4): 171-92.

[26] Egerton TA. Does photoelectrocatalysis by $TiO_2$ work? Journal of Chemical Technology and Biotechnology 2011; 86(8): 1024-31.

[27] Pelaez M, Nolan NT, Pillai SC, et al. A review on the visible light active titanium dioxide photocatalysts for environmental applications. Applied Catalysis B-Environmental 2012; 125: 331-49.

[28] Vinodgopal K, Hotchandani S, Kamat PV. Electrochemically Assisted Photocatalysis-$TiO_2$ Particulate Film Electrodes for Photocatalytic Degradation of 4-Chlorophenol. Journal of Physical Chemistry 1993; 97(35): 9040-4.

[29] Georgieva J, Valova E, Armyanov S, Philippidis N, Poulios I, Sotiropoulos S. Bi-component semiconductor oxide photoanodes for the photoelectrocatalytic oxidation of

organic solutes and vapours: A short review with emphasis to $TiO_2$-$WO_3$ photoanodes. Journal of Hazardous Materials 2012; 211: 30-46.

[30] Rajeshwar K. Photoelectrochemistry and the environment. Journal of Applied Electrochemistry 1995; 25(12): 1067-82.

[31] Finklea HO. Semiconductor electrodes. New York: Elsevier, 1988.

[32] Chong MN, Jin B, Chow CWK, Saint C. Recent developments in photocatalytic water treatment technology: A review. Water Research 2010; 44(10): 2997-3027.

[33] Zhang Y, Xiong X, Han Y, et al. Photoelectrocatalytic degradation of recalcitrant organic pollutants using $TiO_2$ film electrodes: An overview. Chemosphere 2012; 88(2): 145-54.

[34] Rostami I, Juhasz AL. Assessment of Persistent Organic Pollutant (POP) Bioavailability and Bioaccessibility for Human Health Exposure Assessment: A Critical Review. Critical Reviews in Environmental Science and Technology 2011; 41(7): 623-56.

[35] Horáková M, Klementová Š, Kříž P, et al. The synergistic effect of Advanced Oxidation Processes to eliminate resistant chemical compounds.Surface and Coatings Technology.Available at: http://dx.doi.org/10.1016/j.surfcoat.2013.10.068 (accessed 1 February 2014).

[36] Martínez-Huitle CA, Brillas E. Decontamination of wastewaters containing synthetic organic dyes by electrochemical methods: A general review. Applied Catalysis B: Environmental 2009; 87(3-4): 105-45.

[37] Feng L, van Hullebusch ED, Rodrigo MA, Esposito G, Oturan MA. Removal of residual anti-inflammatory and analgesic pharmaceuticals from aqueous systems by electrochemical advanced oxidation processes. A review. Chemical Engineering Journal 2013; 228(0): 944-64.

[38] Shan AY, Ghazi TIM, Rashid SA. Immobilisation of titanium dioxide onto supporting materials in heterogeneous photocatalysis: A review. Applied Catalysis A: General 2010; 389(1-2): 1-8.

[39] Shankar K, Basham JI, Allam NK, et al. Recent Advances in the Use of $TiO_2$ Nanotube and Nanowire Arrays for Oxidative Photoelectrochemistry. Journal of Physical Chemistry C 2009; 113(16): 6327-59.

[40] Carp O, Huisman CL, Reller A. Photoinduced reactivity of titanium dioxide. Progress in Solid State Chemistry 2004; 32(1-2): 33-177.

[41] Shao C, Zhou G, Li Z, Wu Y, Xu D, Sun B. Fabrication of large-diameter tube-like mesoporous $TiO_2$ via homogeneous precipitation and photocatalytic decomposition of papermaking wastewater. Chemical Engineering Journal 2013; 230: 227-35.

[42] He F, Li J, Li T, Li G. Solvothermal synthesis of mesoporous $TiO_2$: The effect of morphology, size and calcination progress on photocatalytic activity in the degradation of gaseous benzene. Chemical Engineering Journal 2014; 237(0): 312-21.

[43] Guaraldo TT, Pulcinelli SH, Zanoni MVB. Influence of particle size on the photoactivity of Ti/$TiO_2$ thin film electrodes, and enhanced photoelectrocatalytic degradation of indigo carmine dye. Journal of Photochemistry and Photobiology A: Chemistry 2011; 217(1): 259-66.

[44] Zubieta CE, Soltero-Martinez JFA, Luengo CV, Schulz PC. Preparation, characterization and photoactivity of $TiO_2$ obtained by a reverse microemulsion route. Powder Technology 2011; 212(3): 410-7.

[45] Rajashekhar KE, Devi LG. Polymorphic phase transformation of Degussa P25 $TiO_2$ by the chelation of diaminopyridine on $TiO_6^{2-}$ octahedron: Correlation of anatase to rutile phase ratio on the photocatalytic activity. Journal of Molecular Catalysis a-Chemical 2013; 374: 12-21.

[46] Andronic L, Duta A. $TiO_2$ thin films for dyes photodegradation. Thin Solid Films 2007; 515(16): 6294-7.

[47] Kim DH, Anderson MA. Photoelectrocatalytic degradation of formic-acid using a porous $TiO_2$ thin-film electrode. Environmental Science & Technology 1994; 28(3): 479-83.

[48] Qin X, Jing L, Tian G, Qu Y, Feng Y. Enhanced photocatalytic activity for degrading Rhodamine B solution of commercial Degussa P25 $TiO_2$ and its mechanisms. Journal of Hazardous Materials 2009; 172(2–3): 1168-74.

[49] Lee H, Song MY, Jurng J, Park Y-K. The synthesis and coating process of $TiO_2$ nanoparticles using CVD process. Powder Technology 2011; 214(1): 64-8.

[50] Rathouský J, Wessels K, Wark M, Oekermann T. Texture properties of nanoporous $TiO_2$ films prepared by anodic electrodeposition using a structure-directing agent. In: From Zeolites to Porous MOF Materials.. Studies in Surface Science and Catalysis, Elsevier2007; 170:1494-501.

[51] Firdaus CM, Rizam MSBS, Rusop M, Hidayah SR. Characterization of ZnO and ZnO: $TiO_2$ Thin Films Prepared by Sol-Gel Spray-Spin Coating Technique. Procedia Engineering 2012; 41(0): 1367-73.

[52] Zanoni MVB, Sene JJ, Anderson MA.Photoelectrocatalytic degradation of Remazol Brilliant Orange 3R on titanium dioxide thin-film electrodes. Journal of Photochemistry and Photobiology A: Chemistry 2003; 157(1): 55-63.

[53] Wu C-Y, Lee Y-L, Lo Y-S, Lin C-J, Wu C-H.Thickness-dependent photocatalytic performance of nanocrystalline $TiO_2$ thin films prepared by sol-gel spin coating. Applied Surface Science 2013; 280: 737-44.

[54] Wang X, Shi F, Gao X, Fan C, Huang W, Feng X. A sol-gel dip/spin coating method to prepare titanium oxide films. Thin Solid Films 2013; 548(0): 34-9.

[55] Mechiakh R, Ben Sedrine N, Chtourou R, Bensaha R. Correlation between microstructure and optical properties of nano-crystalline $TiO_2$ thin films prepared by sol-gel dip coating. Applied Surface Science 2010; 257(3): 670-6.

[56] Vargas-Florencia D, Edvinsson T, Hagfeldt A, Furo I. Pores in nanostructured $TiO_2$ films. Size distribution and pore permeability. Journal of Physical Chemistry C 2007; 111(21): 7605-11.

[57] Gaya UI, Abdullah AH. Heterogeneous photocatalytic degradation of organic contaminants over titanium dioxide: A review of fundamentals, progress and problems. Journal of Photochemistry and Photobiology C: Photochemistry Reviews 2008; 9(1): 1-12.

[58] Carneiro PA, Osugi ME, Sene JJ, Anderson MA, Zanoni MVB. Evaluation of color removal and degradation of a reactive textile azo dye on nanoporous $TiO_2$ thin-film electrodes.ElectrochimicaActa 2004; 49(22-23): 3807-20.

[59] Zhou M, Ma X. Efficient photoelectrocatalytic activity of $TiO_2$/Ti anode fabricated by metalorganic chemical vapor deposition (MOCVD). Electrochemistry Communications 2009; 11(4): 921-4.

[60] Liu Y, Gan X, Zhou B, et al. Photoelectrocatalytic degradation of tetracycline by highly effective $TiO_2$nanopore arrays electrode. Journal of Hazardous Materials 2009; 171(1-3): 678-83.

[61] MonteiroPaschoal FM, Anderson MA, Zanoni MVB.Simultaneous removal of chromium and leather dye from simulated tannery effluent by photoelectrochemistry. Journal of Hazardous Materials 2009; 166(1): 531-7.

[62] Fraga LE, Anderson MA, Beatriz MLPMA, Paschoal FMM, Romao LP, Zanoni MVB. Evaluation of the photoelectrocatalytic method for oxidizing chloride and simultaneous removal of microcystin toxins in surface waters.ElectrochimicaActa 2009; 54(7): 2069-76.

[63] Tang H, Prasad K, Sanjines R, Schmid PE, Levy F. Electrical and optical-properties of $TiO_2$ anatase thin-films. Journal of Applied Physics 1994; 75(4): 2042-7.

[64] Rouquerol J, Avnir D, Everett DH, et al. Guidelines for the characterization of porous solids. Studies in Surface Science and Catalysis 1994; 87: 1-9.

[65] Pan JH, Zhao XS, Lee WI. Block copolymer-templated synthesis of highly organized mesoporous $TiO_2$-based films and their photoelectrochemical applications. Chemical Engineering Journal 2011; 170(2-3): 363-80.

[66] Hepel M, Hazelton S. Photoelectrocatalytic degradation of diazo dyes on nanostructured $WO_3$ electrodes. ElectrochimicaActa 2005; 50(25-26): 5278-91.

[67] Thongsuriwong K, Amornpitoksuk P, Suwanboon S. Structure, morphology, photocatalytic and antibacterial activities of ZnO thin films prepared by sol-gel dip-coating method. Advanced Powder Technology 2013; 24(1): 275-80.

[68] Mahadik MA, Shinde SS, Rajpure KY, Bhosale CH. Photocatalytic oxidation of Rhodamine B with ferric oxide thin films under solar illumination. Materials Research Bulletin 2013; 48(10): 4058-65.

[69] Prakasam HE, Varghese OK, Paulose M, Mor GK, Grimes CA. Synthesis and photoelectrochemical properties of nanoporous iron (III) oxide by potentiostatic anodization. Nanotechnology 2006; 17(17): 4285-91.

[70] Liu X, Wang F, Wang Q. Nanostructure-based $WO_3$ photoanodes for photoelectrochemical water splitting. Physical Chemistry Chemical Physics 2012; 14(22): 7894-911.

[71] Rehman S, Ullah R, Butt AM, Gohar ND. Strategies of making $TiO_2$ and ZnO visible light active. Journal of Hazardous Materials 2009; 170(2-3): 560-9.

[72] Minggu LJ, Daud WRW, Kassim MB. An overview of photocells and photoreactors for photoelectrochemical water splitting. International Journal of Hydrogen Energy 2010; 35(11): 5233-44.

[73] Ahmed S, Rasul MG, Martens WN, Brown R, Hashib MA. Advances in Heterogeneous Photocatalytic Degradation of Phenols and Dyes in Wastewater: A Review. Water Air and Soil Pollution 2011; 215(1-4): 3-29.

[74] Song X-M, Wu J-M, Yan M. Photocatalytic and photoelectrocatalytic degradation of aqueous Rhodamine B by low-temperature deposited anatase thin films. Materials Chemistry and Physics 2008; 112(2): 510-5.

[75] Zainal Z, Lee CY, Hussein MZ, Kassim A, Yusof NA. Electrochemical-assisted photodegradation of dye on $TiO_2$ thin films: investigation on the effect of operational parameters. Journal of Hazardous Materials 2005; 118(1-3): 197-203.

[76] Hashimoto K, Irie H, Fujishima A. $TiO_2$ photocatalysis: A historical overview and future prospects. Japanese Journal of Applied Physics Part 1-Regular Papers Brief Communications & Review Papers 2005; 44(12): 8269-85.

[77] Ni M, Leung MKH, Leung DYC, Sumathy K. A review and recent developments in photocatalytic water-splitting using $TiO_2$ for hydrogen production. Renewable & Sustainable Energy Reviews 2007; 11(3): 401-25.

[78] Wu H, Zhang Z. Photoelectrochemical water splitting and simultaneous photoelectrocatalytic degradation of organic pollutant on highly smooth and ordered $TiO_2$ nanotube arrays. Journal of Solid State Chemistry 2011; 184(12): 3202-7.

[79] Baram N, Starosvetsky D, Starosvetsky J, Epshtein M, Armon R, Ein-Eli Y. Enhanced inactivation of E-coli bacteria using immobilized porous $TiO_2$ photoelectrocatalysis. ElectrochimicaActa 2009; 54(12): 3381-6.

[80] Paschoal FMM, Anderson MA, Zanoni MVB. The photoelectrocatalytic oxidative treatment of textile wastewater containing disperse dyes. Desalination 2009; 249(3): 1350-5.

[81] Mohamed AER, Rohani S. Modified $TiO_2$ nanotube arrays (TNTAs): progressive strategies towards visible light responsive photoanode, a review. Energy & Environmental Science 2011; 4(4): 1065-86.

[82] Iijima S. Helical microtubules of graphitic carbon. Nature 1991; 354(6348): 56-8.

[83] Zhang Z, Yuan Y, Shi G, et al. Photoelectrocatalytic activity of highly ordered $TiO_2$ nanotube arrays electrode for azo dye degradation. Environmental Science & Technology 2007; 41(17): 6259-63.

[84] Zhang Q, Jing Y, Shiue A, et al. Photocatalytic degradation of malathion by $TiO_2$ and Pt-$TiO_2$ nanotube photocatalyst and kinetic study. Journal of Environmental Science and Health Part B-Pesticides Food Contaminants and Agricultural Wastes 2013; 48(8): 686-92.

[85] Liang H-C, Li X-Z. Effects of structure of anodic $TiO_2$ nanotube arrays on photocatalytic activity for the degradation of 2,3-dichlorophenol in aqueous solution. Journal of Hazardous Materials 2009; 162(2-3): 1415-22.

[86] Smith YR, Kar A, Subramanian V. Investigation of Physicochemical Parameters that Influence Photocatalytic Degradation of Methyl Orange over $TiO_2$ Nanotubes. Industrial & Engineering Chemistry Research 2009; 48(23): 10,268-76.

[87] Grandcolas M, Cottineau T, Louvet A, Keller N, Keller V. Solar light-activated photocatalytic degradation of gas phase diethylsulfide on $WO_3$-modified $TiO_2$ nanotubes. Applied Catalysis B-Environmental 2013; 138: 128-40.

[88] Sennik E, Colak Z, Kilinc N, Ozturk ZZ. Synthesis of highly-ordered $TiO_2$ nanotubes for a hydrogen sensor. International Journal of Hydrogen Energy 2010; 35(9): 4420-7.

[89] Zhao R, Xu M, Wang J, Chen G. A pH sensor based on the $TiO_2$ nanotube array modified Ti electrode. Electrochimica Acta 2010; 55(20): 5647-51.

[90] Mun K-S, Alvarez SD, Choi W-Y, Sailor MJ. A Stable, Label-free Optical Interferometric Biosensor Based on $TiO_2$ Nanotube Arrays.Acs. Nano 2010; 4(4): 2070-6.

[91] Mor GK, Shankar K, Paulose M, Varghese OK, Grimes CA. Use of highly-ordered $TiO_2$ nanotube arrays in dye-sensitized solar cells. Nano Letters 2006; 6(2): 215-8.

[92] Patrick CE, Giustino F. Structural and Electronic Properties of Semiconductor-Sensitized Solar-Cell Interfaces. Advanced Functional Materials 2011; 21(24): 4663-7.

[93] Park JH, Kim S, Bard AJ. Novel carbon-doped $TiO_2$ nanotube arrays with high aspect ratios for efficient solar water splitting. Nano Letters 2006; 6(1): 24-8.

[94] Grimes CA, Mor GK. $TiO_2$ nanotube arrays: Synthesis, Properties, and Applications. New York: Springer, 2009.

[95] Zhang Q, Ackerman E, Li Y. Photocatalytic reduction of $CO_2$ to fuels by novel $TiO_2$ nanotubes. Abstracts of Papers of the American Chemical Society 2011; 241.

[96] Popat KC, Eltgroth M, La Tempa TJ, Grimes CA, Desai TA. Titania nanotubes: A novel platform for drug-eluting coatings for medical implants. Small 2007; 3(11): 1878-81.

[97] Popat KC, Leoni L, Grimes CA, Desai TA. Influence of engineered titaniananotubular surfaces on bone cells. Biomaterials 2007; 28(21): 3188-97.

[98] Miao Z, Xu DS, Ouyang JH, Guo GL, Zhao XS, Tang YQ. Electrochemically induced sol-gel preparation of single-crystalline $TiO_2$ nanowires. Nano Letters 2002; 2(7): 717-20.

[99] Yu J, Yu H, Cheng B, Zhao X, Zhang Q. Preparation and photocatalytic activity of mesoporous anatase $TiO_2$nanofibers by a hydrothermal method. Journal of Photochemistry and Photobiology A: Chemistry 2006; 182(2): 121-7.

[100] Liu B, Aydil ES.Growth of Oriented Single-Crystalline Rutile $TiO_2$Nanorods on Transparent Conducting Substrates for Dye-Sensitized Solar Cells. Journal of the American Chemical Society 2009; 131(11): 3985-90.

[101] Wu JJ, Yu CC. Aligned $TiO_2$nanorods and nanowalls. Journal of Physical Chemistry B 2004; 108(11): 3377-9.

[102] Zhu K, Neale NR, Miedaner A, Frank AJ.Enhanced charge-collection efficiencies and light scattering in dye-sensitized solar cells using oriented $TiO_2$ nanotubes arrays. Nano Letters 2007; 7(1): 69-74.

[103] Liu Z, Zhang X, Nishimoto S, et al. Highly ordered $TiO_2$ nanotube arrays with controllable length for photoelectrocatalytic degradation of phenol. Journal of Physical Chemistry C 2008; 112(1): 253-9.

[104] Grimes CA. Synthesis and application of highly ordered arrays of $TiO_2$ nanotubes. Journal of Materials Chemistry 2007; 17(15): 1451-7.

[105] Mor GK, Varghese OK, Paulose M, Shankar K, Grimes CA. A review on highly ordered, vertically oriented $TiO_2$ nanotube arrays: Fabrication, material properties, and solar energy applications. Solar Energy Materials and Solar Cells 2006; 90(14).

[106] Macak JM, Tsuchiya H, Ghicov A, et al. $TiO_2$ nanotubes: Self-organized electrochemical formation, properties and applications. Current Opinion in Solid State & Materials Science 2007; 11(1-2).

[107] Nah Y-C, Paramasivam I, Schmuki P. Doped $TiO_2$ and $TiO_2$ Nanotubes: Synthesis and Applications. Chemphyschem 2010; 11(13): 2698-713.

[108] Ou H-H, Lo S-L. Review of titania nanotubes synthesized via the hydrothermal treatment: Fabrication, modification, and application. Separation and Purification Technology 2007; 58(1): 179-91.

[109] Zhang M, Bando Y, Wada K. Sol-gel template preparation of $TiO_2$ nanotubes and nanorods. Journal of Materials Science Letters 2001; 20(2): 167-70.

[110] Bavykin DV, Friedrich JM, Walsh FC. Protonated titanates and $TiO_2$ nanostructured materials: Synthesis, properties, and applications. Advanced Materials 2006; 18(21): 2807-24.

[111] Zwilling V, Darque-Ceretti E, Boutry-Forveille A, David D, Perrin MY, Aucouturier M. Structure and physicochemistry of anodic oxide films on titanium and TA6V alloy. Surface and Interface Analysis 1999; 27(7): 629-37.

[112] Gong D, Grimes CA, Varghese OK, et al. Titanium oxide nanotube arrays prepared by anodic oxidation. Journal of Materials Research 2001; 16(12): 3331-4.

[113] Cai QY, Paulose M, Varghese OK, Grimes CA. The effect of electrolyte composition on the fabrication of self-organized titanium oxide nanotube arrays by anodic oxidation. Journal of Materials Research 2005; 20(1): 230-6.

[114] Ruan CM, Paulose M, Varghese OK, Mor GK, Grimes CA. Fabrication of highly ordered $TiO_2$ nanotube arrays using an organic electrolyte. Journal of Physical Chemistry B 2005; 109(33): 15,754-9.

[115] Paulose M, Shankar K, Yoriya S, et al. Anodic growth of highly ordered $TiO_2$ nanotube arrays to 134 μm in length. Journal of Physical Chemistry B 2006; 110(33): 16,179-84.

[116] Paulose M, Prakasam HE, Varghese OK, et al. $TiO_2$ nanotube arrays of 1000 μm length by anodization of titanium foil: Phenol red diffusion. Journal of Physical Chemistry C 2007; 111(41): 14,992-7.

[117] Shankar K, Mor GK, Fitzgerald A, Grimes CA. Cation effect on the electrochemical formation of very high aspect ratio $TiO_2$ nanotube arrays in formamide-Water mixtures. Journal of Physical Chemistry C 2007; 111(1): 21-6.

[118] Richter C, Wu Z, Panaitescu E, Willey RJ, Menon L. Ultrahigh-aspect-ratio titania nanotubes. Advanced Materials 2007; 19(7): 946-948.

[119] Allam NK, Grimes CA. Formation of vertically oriented $TiO_2$ nanotube arrays using a fluoride free HCl aqueous electrolyte. Journal of Physical Chemistry C 2007; 111(35): 13,028-32.

[120] Mor GK, Varghese OK, Paulose M, Mukherjee N, Grimes CA. Fabrication of tapered, conical-shaped titania nanotubes. Journal of Materials Research 2003; 18(11): 2588-93.

[121] Bauer S, Kleber S, Schmuki P. $TiO_2$ nanotubes: Tailoring the geometry in $H_3PO_4$/HF electrolytes. Electrochemistry Communications 2006; 8(8): 1321-5.

[122] LaTempa TJ, Feng X, Paulose M, Grimes CA. Temperature-Dependent Growth of Self-Assembled Hematite (alpha-Fe2O3) Nanotube Arrays: Rapid Electrochemical Synthesis and Photoelectrochemical Properties. Journal of Physical Chemistry C 2009; 113(36): 16,293-8.

[123] Lai CW, Abd Hamid SB, Sreekantan S. A Novel Solar Driven Photocatalyst: Well-Aligned Anodic $WO_3$ Nanotubes. International Journal of Photoenergy 2013; 2013. doi:10.1155/2013/745301 (accessed 25 November 2013).

[124] Park J, Kim K, Choi J. Formation of ZnO nanowires during short durations of potentiostatic and galvanostatic anodization. Current Applied Physics 2013; 13(7): 1370-5.

[125] Ghicov A, Schmidt B, Kunze J, Schmuki P. Photoresponse in the visible range from Cr doped $TiO_2$ nanotubes. Chemical Physics Letters 2007; 433(4-6): 323-6.

[126] Ferreira VC, Nunes MR, Silvestre AJ, Monteiro OC. Synthesis and properties of Co-doped titanate nanotubes and their optical sensitization with methylene blue. Materials Chemistry and Physics 2013; 142(1): 355-62.

[127] Gong J, Pu W, Yang C, Zhang J. Novel one-step preparation of tungsten loaded $TiO_2$ nanotube arrays with enhanced photoelectrocatalytic activity for pollutant degradation and hydrogen production. Catalysis Communications 2013; 36: 89-93.

[128] Li Y, Xiang Y, Peng S, Wang X, Zhou L. Modification of Zr-doped titania nanotube arrays by urea pyrolysis for enhanced visible-light photoelectrochemical H-2 generation. ElectrochimicaActa 2013; 87: 794-800.

[129] Xu Z, Yu J. Visible-light-induced photoelectrochemical behaviors of Fe-modified $TiO_2$ nanotube arrays.Nanoscale 2011; 3(8): 3138-44.

[130] Sun L, Cai J, Wu Q, Huang P, Su Y, Lin C. N-doped $TiO_2$ nanotube array photoelectrode for visible-light-induced photoelectrochemical and photoelectrocatalytic activities. Electrochimica Acta 2013; 108(0): 525-31.

[131] Yu Y, Wu H-H, Zhu B-L, et al. Preparation, characterization and photocatalytic activities of F-doped $TiO_2$ nanotubes. Catalysis Letters 2008; 121(1-2): 165-71.

[132] Yan G, Zhang M, Hou J, Yang J. Photoelectrochemical and photocatalytic properties of N plus S co-doped $TiO_2$ nanotube array films under visible light irradiation. Materials Chemistry and Physics 2011; 129(1-2): 553-7.

[133] Lu N, Zhao H, Li J, Quan X, Chen S. Characterization of boron-doped $TiO_2$ nanotube arrays prepared by electrochemical method and its visible light activity. Separation and Purification Technology 2008; 62(3): 668-73.

[134] Paramasivalm I, Macak JM, Schmuki P. Photocatalytic activity of $TiO_2$-nanotube layers loaded with Ag and Au nanoparticles. Electrochemistry Communications 2008; 10(1): 71-5.

[135] Li J, Lin C-J, Li J-T, Lin Z-Q. A photoelectrochemical study of CdS modified $TiO_2$ nanotube arrays as photoanodes for cathodic protection of stainless steel. Thin Solid Films 2011; 519(16): 5494-502.

[136] Gan J, Zhai T, Lu X, Xie S, Mao Y, Tong Y. Facile preparation and photoelectrochemical properties of CdSe/$TiO_2$ NTAs. Materials Research Bulletin 2012; 47(3): 580-5.

[137] Sakthivel S, Shankar MV, Palanichamy M, Arabindoo B, Bahnemann DW, Murugesan V. Enhancement of photocatalytic activity by metal deposition: characterisation and photonic efficiency of Pt, Au and Pd deposited on $TiO_2$ catalyst. Water Research 2004; 38(13): 3001-8.

[138] Henglein A. Photochemistry of colloidal cadmium-sulfide.2.Effects of adsorbed methyl viologen and of colloidal platinum. Journal of Physical Chemistry 1982; 86(13): 2291-3.

[139] Shankar K, Tep KC, Mor GK, Grimes CA. An electrochemical strategy to incorporate nitrogen in nanostructured $TiO_2$ thin films: modification of bandgap and photoelectrochemical properties. Journal of Physics D-Applied Physics 2006; 39(11): 2361-6.

[140] Antony RP, Mathews T, Ajikumar PK, Krishna DN, Dash S, Tyagi AK. Electrochemically synthesized visible light absorbing vertically aligned N-doped $TiO_2$ nanotube array films. Materials Research Bulletin 2012; 47(12): 4491-7.

[141] Zhou X-y, Shao J, Wan B.A One-Step Electrochemical Method for the Production of $TiO_{2-x}N_x$ Nanotubes. Journal of the Electrochemical Society 2013; 160(6): H335-H7.

[142] Kim D, Fujimoto S, Schmuki P, Tsuchiya H. Nitrogen doped anodic $TiO_2$ nanotubes grown from nitrogen-containing Ti alloys. Electrochemistry Communications 2008; 10(6): 910-3.

[143] Su Y, Zhang X, Zhou M, Han S, Lei L. Preparation of high efficient photoelectrode of N-F-codoped $TiO_2$ nanotubes. Journal of Photochemistry and Photobiology A: Chemistry 2008; 194(2-3): 152-60.

[144] Xua Z, Yanga W, Lia Q, Gaoa S, Shanga JK. Passivated n–p co-doping of niobium and nitrogen into self-organized $TiO_2$ nanotube arrays for enhanced visible light photocatalytic performance.2014; 144: 343-52.

[145] Liu H, Liu G, Shi X. N/Zr-codoped $TiO_2$ nanotube arrays: Fabrication, characterization, and enhanced photocatalytic activity. Colloids and Surfaces a-Physicochemical and Engineering Aspects 2010; 363(1-3): 35-40.

[146] Milad AMH, Minggu LJ, Kassim MB, Daud WRW. Carbon doped $TiO_2$ nanotubes photoanodes prepared by in-situ anodic oxidation of Ti-foil in acidic and organic medium with photocurrent enhancement. Ceramics International 2013; 39(4): 3731-9.

[147] Krengvirat W, Sreekantan S, Noor A-FM, et al. Carbon-incorporated $TiO_2$photoelectrodes prepared via rapid-anodic oxidation for efficient visible-light hydrogen generation. International Journal of Hydrogen Energy 2012; 37(13): 10,046-56.

[148] Li J, Lu N, Quan X, Chen S, Zhao H. Facile method for fabricating boron-doped $TiO_2$ nanotube array with enhanced photoelectrocatalytic properties. Industrial & Engineering Chemistry Research 2008; 47(11): 3804-8.

[149] Zhou X, Peng F, Wang H, Yu H, Yang J. Preparation of B,N-codoped nanotube arrays and their enhanced visible light photoelectrochemical performances. Electrochemistry Communications 2011; 13(2): 121-4.

[150] Ruan CM, Paulose M, Varghese OK, Grimes CA. Enhanced photo electrochemical-response in highly ordered $TiO_2$ nanotube-arrays anodized in boric acid containing electrolyte. Solar Energy Materials and Solar Cells 2006; 90(9): 1283-95.

[151] Das C, Paramasivam I, Liu N, Schmuki P. Photoelectrochemical and photocatalytic activity of tungsten doped $TiO_2$ nanotube layers in the near visible region. ElectrochimicaActa 2011; 56(28): 10,557-61.

[152] Sun M, Cui X. Anodically grown Si-W codoped $TiO_2$ nanotubes and its enhanced visible light photoelectrochemical response. Electrochemistry Communications 2012; 20: 133-6.

[153] Liu H, Liu G, Zhou Q. Preparation and characterization of Zr doped $TiO_2$ nanotube arrays on the titanium sheet and their enhanced photocatalytic activity. Journal of Solid State Chemistry 2009; 182(12): 3238-42.

[154] Nie J, Mo Y, Zheng B, Yuan H, Xiao D. Electrochemical fabrication of lanthanum-doped $TiO_2$ nanotube array electrode and investigation of its photoelectrochemical capability. ElectrochimicaActa 2013; 90: 589-96.

[155] Xie K, Sun L, Wang C, et al. Photoelectrocatalytic properties of Ag nanoparticles loaded $TiO_2$ nanotube arrays prepared by pulse current deposition. ElectrochimicaActa 2010; 55(24): 7211-8.

[156] Zhang S, Peng F, Wang H, et al. Electrodeposition preparation of Ag loaded N-doped $TiO_2$nanotube arrays with enhanced visible light photocatalytic performance. Catalysis Communications 2011; 12(8): 689-93.

[157] Xing L, Jia J, Wang Y, Zhang B, Dong S. Pt modified $TiO_2$ nanotubes electrode: Preparation and electrocatalytic application for methanol oxidation. International Journal of Hydrogen Energy 2010; 35(22): 12,169-73.

[158] Yin Y, University T, Tan X, et al. Efficient synthesis of titania nanotubes and enhanced photoresponse of Pt decorated $TiO_2$ for water splitting. Frontiers of Chemical Engineering in China 2013; 3(3): 298-304.

[159] Qin Y-H, Yang H-H, Lv R-L, Wang W-G, Wang C-W.$TiO_2$ nanotube arrays supported Pd nanoparticles for ethanol electrooxidation in alkaline media. ElectrochimicaActa 2013; 106: 372-7.

[160] Cheng X, Liu H, Chen Q, Li J, Wang P. Preparation and characterization of palladium nano-crystallite decorated $TiO_2$nano-tubes photoelectrode and its enhanced photocatalytic efficiency for degradation of diclofenac. Journal of Hazardous Materials 2013; 254: 141-8.

[161] Zhang X, Lin S, Liao J, et al. Uniform deposition of water-soluble CdS quantum dots on $TiO_2$ nanotube arrays by cyclic voltammetric electrodeposition: Effectively prevent aggregation and enhance visible-light photocatalytic activity. 2013; 108: 296-303.

[162] Feng H, Tran TT, Chen L, Yuan L, Cai Q. Visible light-induced efficiently oxidative decomposition of p-Nitrophenol by CdTe/$TiO_2$ nanotube arrays. Chemical Engineering Journal 2013; 215: 591-9.

[163] Tsui L-k, Zangari G. Modification of $TiO_2$ nanotubes by $Cu_2O$ for photoelectrochemical, photocatalytic, and photovoltaic devices. 2013. http://dx.doi.org/10.1016/j.electacta.2013.09.150 (accessed 1 January 2014).

[164] Asahi R, Morikawa T, Ohwaki T, Aoki K, Taga Y. Visible-light photocatalysis in nitrogen-doped titanium oxides. Science 2001; 293(5528): 269-71.

[165] Li S, Lin S, Liao J, Pan N, Li D, Li J. Nitrogen-Doped $TiO_2$ Nanotube Arrays with Enhanced Photoelectrochemical Property. International Journal of Photoenergy 2012; 2012. http://dx.doi.org/10.1155/2012/794207 (accessed 01 January 2014).

[166] Serpone N. Is the band gap of pristine $TiO_2$ narrowed by anion-and cation-doping of titanium dioxide in second-generation photocatalysts? Journal of Physical Chemistry B 2006; 110(48): 24,287-93.

[167] Zhao X, Guo L, Hu C, Liu H, Qu J. Simultaneous destruction of Nickel (II)-EDTA with $TiO_2$/Ti film anode and electrodeposition of nickel ions on the cathode. Applied Catalysis B: Environmental 2014; 144(0): 478-85.

[168] Tahir M, Amin NS.Advances in visible light responsive titanium oxide-based photocatalysts for $CO_2$ conversion to hydrocarbon fuels. Energy Conversion and Management 2013; 76(0): 194-214.

[169] Quan X, Ruan X, Zhao H, Chen S, Zhao Y. Photoelectrocatalytic degradation of pentachlorophenol in aqueous solution using a $TiO_2$ nanotube film electrode. Environmental Pollution 2007; 147(2): 409-14.

[170] Quan X, Yang SG, Ruan XL, Zhao HM. Preparation of titania nanotubes and their environmental applications as electrode. Environmental Science & Technology 2005; 39(10): 3770-5.

[171] Philippidis N, Sotiropoulos S, Efstathiou A, Poulios I. Photoelectrocatalytic degradation of the insecticide imidacloprid using $TiO_2$/Ti electrodes. Journal of Photochemistry and Photobiology A: Chemistry 2009; 204(2-3): 129-36.

[172] Fang T, Yang C, Liao L. Photoelectrocatalytic degradation of high COD dipterex pesticide by using $TiO_2$/Ni photo electrode. Journal of Environmental Sciences-China 2012; 24(6): 1149-56.

[173] Chang H-S, Choo K-H, Lee B, Choi S-J.The methods of identification, analysis, and removal of endocrine disrupting compounds (EDCs) in water. Journal of Hazardous Materials 2009; 172(1): 1-12.

[174] Daghrir R, Drogui P, Dimboukou-Mpira A, El Khakani MA.Photoelectrocatalytic degradation of carbamazepine using Ti/$TiO_2$ nanostructured electrodes deposited by means of a pulsed laser deposition process. Chemosphere 2013; 93(11): 2756-66.

[175] Liu H, Liu G, Fan J, et al. Photoelectrocatalytic degradation of 4,4'-dibromobiphenyl in aqueous solution on $TiO_2$ and doped $TiO_2$ nanotube arrays. Chemosphere 2011; 82(1): 43-7.

[176] Martinez-Huitle CA, Brillas E. Decontamination of wastewaters containing synthetic organic dyes by electrochemical methods: A general review. Applied Catalysis B: Environmental 2009; 87(3-4): 105-45.

[177] Jurado-Sanchez B, Ballesteros E, Gallego M. Occurrence of aromatic amines and N-nitrosamines in the different steps of a drinking water treatment plant. Water Research 2012; 46(14): 4543-55.

[178] Egerton TA, Christensen PA, Kosa SAM, Onoka B, Harper JC, Tinlin JR. Photoelectrocatalysis by titanium dioxide for water treatment. International Journal of Environment and Pollution 2006; 27(1-3): 2-19.

[179] Pardeshi SK, Patil AB. Solar photocatalytic degradation of resorcinol a model endocrine disrupter in water using zinc oxide. Journal of Hazardous Materials 2009; 163(1): 403-9.

[180] Stasinakis AS, Kordoutis CI, Tsiouma VC, Gatidou G, Thomaidis NS.Removal of selected endocrine disrupters in activated sludge systems: Effect of sludge retention time on their sorption and biodegradation. Bioresource Technology 2010; 101(7): 2090-5.

[181] Balest L, Lopez A, Mascolo G, Di Iaconi C. Removal of endocrine disrupter compounds from municipal wastewater using an aerobic granular biomass reactor. Biochemical Engineering Journal 2008; 41(3): 288-94.

[182] Zheng Q, Lee C. Visible light photoelectrocatalytic degradation of methyl orange using anodized nanoporous $WO_3$. ElectrochimicaActa 2014; 115(0): 140-5.

[183] Li J, Zheng L, Li L, Xian Y, Jin L. Fabrication of $TiO_2$/Ti electrode by laser-assisted anodic oxidation and its application on photoelectrocatalytic degradation of methylene blue. Journal of Hazardous Materials 2007; 139(1): 72-8.

[184] Song H, Shang J, Zhu T, Ye J, Li Q, Teng F.The improved photoelectrocatalytic degradation of rhodamine B driven by the half-rectified square wave.Electrochimica Acta 2013; 102: 375-80.

[185] Osugi ME, Rajeshwar K, Ferraz ERA, de Oliveira DP, Araújo ÂR, Zanoni MVB. Comparison of oxidation efficiency of disperse dyes by chemical and photoelectrocatalytic chlorination and removal of mutagenic activity. Electrochimica Acta 2009; 54(7): 2086-93.

[186] Guaraldo TT, Zanoni TB, de Torresi SIC, et al. On the application of nanostructured electrodes prepared by Ti/$TiO_2$/$WO_3$"template": A case study of removing toxicity of indigo using visible irradiation. Chemosphere 2013; 91(5): 586-93.

[187] Carneiro PA, Oliveira DP, Umbuzeiro GA, Boldrin Zanoni MV. Mutagenic activity removal of selected disperse dye by photoeletrocatalytic treatment. Journal of Applied Electrochemistry 2010; 40(3): 485-92.

[188] Pelaez M, Nolan NT, Pillai SC, et al.A review on the visible light active titanium dioxide photocatalysts for environmental applications. Applied Catalysis B: Environmental 2012; 125(0): 331-49.

[189] Olya ME, Pirkarami A. Cost-effective photoelectrocatalytic treatment of dyes in a batch reactor equipped with solar cells. Separation and Purification Technology 2013; 118(0): 557-66.

[190] Liu Y, Zhou H, Zhou B, et al. Highly stable CdS-modified short $TiO_2$ nanotube array electrode for efficient visible-light hydrogen generation. International Journal of Hydrogen Energy 2011; 36(1): 167-74.

[191] MonteiroPaschoal FM, Pepping G, Boldrin Zanoni MV, Anderson MA. Photoelectrocatalytic Removal of Bromate Using Ti/$TiO_2$ Coated as a Photocathode. Environmental Science & Technology 2009; 43(19): 7496-502.

[192] Su Y, Han S, Zhang X, Chen X, Lei L. Preparation and visible-light-driven photoelectrocatalytic properties of boron-doped $TiO_2$ nanotubes. Materials Chemistry and Physics 2008; 110(2-3): 239-46.

[193] Xin Y, Liu H, Han L, Zhou Y. Comparative study of photocatalytic and photoelectrocatalytic properties of alachlor using different morphology $TiO_2$/Ti photoelectrodes. Journal of Hazardous Materials 2011; 192(3): 1812-8.

[194] Palmas S, Da Pozzo A, Mascia M, et al. Effect of the preparation conditions on the performance of $TiO_2$ nanotube arrays obtained by electrochemical oxidation. International Journal of Hydrogen Energy 2011; 36(15): 8894-901.

[195] Li Y, Yu H, Song W, Li G, Yi B, Shao Z. A novel photoelectrochemical cell with self-organized $TiO_2$ nanotubes as photoanodes for hydrogen generation. International Journal of Hydrogen Energy 2011; 36(22): 14,374-80.

[196] Sun K-C, Chen Y-C, Kuo M-Y, et al. Synthesis and characterization of highly ordered $TiO_2$ nanotube arrays for hydrogen generation via water splitting. Materials Chemistry and Physics 2011; 129(1-2): 35-9.

[197] Zhang Z, Hossain MF, Takahashi T. Photoelectrochemical water splitting on highly smooth and ordered $TiO_2$ nanotube arrays for hydrogen generation. International Journal of Hydrogen Energy 2010; 35(16): 8528-35.

[198] Cheng X, Pan G, Yu X, Zheng T. Preparation of CdS NCs decorated $TiO_2$nano-tubes arrays photoelectrode and its enhanced photoelectrocatalytic performance and mechanism. Electrochimica Acta 2013; 105: 535-41.

[199] Yang E-l, Shi J-j, LiangH-c, Cheuk W-K. Coaxial $WO_3/TiO_2$ nanotubes/nanorods with high visible light activity for the photodegradation of 2,3-dichlorophenol. Chemical Engineering Journal 2011; 174(2-3): 539-45.

[200] Fraga LE, Franco JH, Orlandi MO, Zanoni MVB.Photoelectrocatalytic oxidation of hair dye basic red 51 at $W/WO_3/TiO_2$bicomposite photoanode activated by ultraviolet and visible radiation. Journal of Environmental Chemical Engineering 2013; 1(3): 194-9.

[201] Cong Y, Li Z, Zhang Y, Wang Q, Xu Q. Synthesis of alpha-$Fe_2O_3/TiO_2$ nanotube arrays for photoelectro-Fenton degradation of phenol. Chemical Engineering Journal 2012; 191: 356-63.

[202] Lin C-J, Lu Y-T, Hsieh C-H, Chien S-H. Surface modification of highly ordered $TiO_2$ nanotube arrays for efficient photoelectrocatalytic water splitting. Applied Physics Letters 2009; 94(11).

[203] Sun L, Cai J, Wu Q, Huang P, Su Y, Lin C. N-doped $TiO_2$ nanotube array photoelectrode for visible-light-induced photoelectrochemical and photoelectrocatalytic activities. ElectrochimicaActa 2013; 108: 525-31.

[204] Wu H, Zhang Z. High photoelectrochemical water splitting performance on nitrogen doped double-wall $TiO_2$ nanotube array electrodes. International Journal of Hydrogen Energy 2011; 36(21): 13481-7.

[205] Rauf MA, Meetani MA, Hisaindee S. An overview on the photocatalytic degradation of azo dyes in the presence of $TiO_2$ doped with selective transition metals. Desalination 2011; 276(1-3): 13-27.

[206] Zhang Z, Yu Y, Wang P. Hierarchical Top-Porous/Bottom-Tubular $TiO_2$ Nanostructures Decorated with Pd Nanoparticles for Efficient Photoelectrocatalytic Decomposition of Synergistic Pollutants. Acs. Applied Materials & Interfaces 2012; 4(2): 990-6.

[207] Li Z, Cui X, Lin Y. Electrochemically Synthesized Ordered $TiO_2$ and Platinum Nanocomposite Electrode: Preparation, Characterization, and Application to Photoelectrocatalytic Methanol Oxidation. Journal of Nanoscience and Nanotechnology 2009; 9(4): 2297-302.

[208] Ye M, Gong J, Lai Y, Lin C, Lin Z. High-Efficiency Photoelectrocatalytic Hydrogen Generation Enabled by Palladium Quantum Dots-Sensitized $TiO_2$ Nanotube Arrays. Journal of the American Chemical Society 2012; 134(38): 15,720-3.

[209] Kang Q, Lu QZ, Liu SH, et al.A ternary hybrid CdS/Pt-$TiO_2$ nanotube structure for photoelectrocatalytic bactericidal effects on Escherichia Coli. Biomaterials 2010; 31(12): 3317-26.

[210] Seferlis AK, Neophytides SG.On the kinetics of photoelectrocatalytic water splitting on nanocrystalline $TiO_2$ films. Applied Catalysis B-Environmental 2013; 132: 543-52.

[211] Palmas S, Mascia M, Vacca A, Tredici I. Photoelectrocatalytic Performances of Nanostructured/Decorated $TiO_2$ Electrodes: Effect of Wavelength and Cell Configuration. International Journal of Photoenergy 2013; 2013. http://dx.doi.org/10.1155/2013/173760 (accessed 1 February 2014).

[212] Selcuk H. Disinfection and formation of disinfection by-products in a photoelectrocatalytic system. Water Research 2010; 44(13): 3966-72.

[213] Gong J, Yang C, Pu W, Zhang J. Liquid phase deposition of tungsten doped $TiO_2$ films for visible light photoelectrocatalytic degradation of dodecyl-benzenesulfonate. Chemical Engineering Journal 2011; 167(1): 190-7.

[214] Gong J, Pu W, Yang C, Zhang J. Tungsten and nitrogen co-doped $TiO_2$ electrode sensitized with Fe-chlorophyllin for visible light photoelectrocatalysis. Chemical Engineering Journal 2012; 209:94-101.

[215] Daghrir R, Drogui P, Delegan N, El Khakani MA.Electrochemical degradation of chlortetracycline using N-doped Ti/$TiO_2$ photoanode under sunlight irradiations. Water Research 2013; 47(17): 6801-10.

[216] Xie Y-B, Li X-Z. Degradation of bisphenolA in aqueous solution by $H2O_2$-assisted photoelectrocatalytic oxidation. Journal of Hazardous Materials 2006; 138(3): 526-33.

[217] Daghrir R, Drogui P, Delegan N, El Khakani MA.Removal of chlortetracycline from spiked municipal wastewater using a photoelectrocatalytic process operated under sunlight irradiations. Science of The Total Environment 2014; 466-467(0): 300-5.

[218] Lei J, Li X, Li W, Sun F, Lu D, Yi J. Arrayed porous iron-doped $TiO_2$ as photoelectrocatalyst with controllable pore size. International Journal of Hydrogen Energy 2011; 36(14): 8167-72.

[219] Gan WY, Friedmann D, Amal R, Zhang S, Chiang K, Zhao H. A comparative study between photocatalytic and photoelectrocatalytic properties of Pt deposited $TiO_2$ thin films for glucose degradation. Chemical Engineering Journal 2010; 158(3): 482-8.

[220] Antoniadou M, Daskalaki VM, Balis N, Kondarides DI, Kordulis C, Lianos P. Photocatalysis and photoelectrocatalysis using (CdS-ZnS)/$TiO_2$ combined photocatalysts. Applied Catalysis B-Environmental 2011; 107(1-2): 188-96.

[221] Christensen PA, Egerton TA, Lin WF, Meynet P, Shao ZG, Wright NG.A novel electrochemical device for the disinfection of fluids by OH radicals. Chemical Communications 2006; (38): 4022-3.

[222] Yu H, Chen S, Quan X, Zhao H, Zhang Y. Silicon nanowire/$TiO_2$ heterojunction arrays for effective photoelectrocatalysis under simulated solar light irradiation. Applied Catalysis B-Environmental 2009; 90(1-2): 242-8.

[223] Su J, Yu H, Chen S, Quan X, Zhao Q. Visible-light-driven photocatalytic and photoelectrocatalytic debromination of BDE-47 on a macroporous silicon/grapheneheterostructure. Separation and Purification Technology 2012; 96: 154-60.

[224] Wang X, Li G, Zhu H, Yu JC, Xiao X, Li Q. Vertically aligned CdTe nanotube arrays on indium tin oxide for visible-light-driven photoelectrocatalysis. Applied Catalysis B: Environmental 2014; 147(0): 17-21.

[225] Scott-Emuakpor EO, Kruth A, Todd MJ, Raab A, Paton GI, Macphee DE. Remediation of 2,4-dichlorophenol contaminated water by visible light-enhanced $WO_3$ photoelectrocatalysis. Applied Catalysis B: Environmental 2012; 123: 433-9.

[226] Zanoni MVB, Guaraldo T. Photoelectrochemical Hydrogen Generation and Concomitant Organic Dye Oxidation under $TiO_2$ Nanotube. ECS transactions 2013; 50(36): 63-70.

INTECH